1-1-2019

# 3D Formation Control in Multi-Robot Teams Using Artificial Potential Fields

Sanjana Reddy Mohan
*University of Denver*

# 3D Formation Control in Multi-Robot Teams Using Artificial Potential Fields


## Abstract

Multi-robot teams find applications in emergency response, search and rescue operations, convoy support and many more. Teams of autonomous aerial vehicles can also be used to protect a cargo of airplanes by surrounding them in some geometric shape. This research develops a control algorithm to attract UAVs to one or a set of bounded geometric shapes while avoiding collisions, re-configuring in the event of departure or addition of UAVs and maneuvering in mission space while retaining the configuration. Using potential field theory, weighted vector fields are described to attract UAVs to a desired formation. In order to achieve this, three vector fields are defined: one attracts UAVs located outside the formation towards bounded geometric shape; one pushes them away from the center towards the desired region and the third controls collision avoidance and dispersion of UAVs within the formation. The result is a control algorithm that is theoretically justified and verified using MATLAB which generates velocity vectors to attract UAVs to a loose formation and maneuver in the mission space while remaining in formation. This approach efficiently scales to different team sizes.



## Document Type

Thesis

## Degree Name

M.S.

## Department

Engineering

## First Advisor

Matthew J. Rutherford, Ph.D.

## Second Advisor

Kimon P. Valavanis, Ph.D.

## Keywords

Multi-robot, Potential fields, Teams, Unmanned aerial vehicles

## Subject Categories

Computer Engineering | Engineering | Robotics

# 3D Formation Control in Multi-Robot Teams Using Artificial Potential Fields

---

A Thesis

Presented to

the Faculty of the Daniel Felix Ritchie School of Engineering and Computer Science

University of Denver

---

In Partial Fulfillment

of the Requirements for the Degree

Master of Science

---

by

Sanjana Reddy Mohan

June 2019

Advisors: Kimon P. Valavanis, Ph.D. and Matthew J. Rutherford, Ph.D.

Author: Sanjana Reddy Mohan
Title: 3D Formation Control in Multi-Robot Teams Using Artificial Potential Fields
Advisors: Kimon P. Valavanis, Ph.D. and Matthew J. Rutherford, Ph.D.
Degree Date: June 2019

# Abstract

Multi-robot teams find applications in emergency response, search and rescue operations, convoy support and many more. Teams of autonomous aerial vehicles can also be used to protect a cargo of airplanes by surrounding them in some geometric shape. This research develops a control algorithm to attract UAVs to one or a set of bounded geometric shapes while avoiding collisions, re-configuring in the event of departure or addition of UAVs and maneuvering in mission space while retaining the configuration. Using potential field theory, weighted vector fields are described to attract UAVs to a desired formation. In order to achieve this, three vector fields are defined: one attracts UAVs located outside the formation towards bounded geometric shape; one pushes them away from the center towards the desired region and the third controls collision avoidance and dispersion of UAVs within the formation. The result is a control algorithm that is theoretically justified and verified using MATLAB which generates velocity vectors to attract UAVs to a loose formation and maneuver in the mission space while remaining in formation. This approach efficiently scales to different team sizes.

# Acknowledgments

I would like to thank my parents, Mohan and Nalini, my brother Sanchith, my husband Rahul and all my family and friends for their love and support without which this research would not have been possible.

I am profoundly grateful to my advisers, Dr. Valavanis and Dr. Rutherford for their guidance throughout this research. I would also like to thank all those at University of Denver who helped me complete this thesis. I extend my gratitude to all my colleagues at the University of Denver Unmanned Systems Research Institute.

# Table of Contents

# List of Tables

# List of Figures

# Chapter 1

# Introduction

Research and development focus on robotics has witnessed a shift to multi-robot systems since the late 1980's. A major objective has been to tackle problems requiring spatio-temporal task scheduling and execution. In such scenarios, each robot in a multi-robot team, equipped with a dedicated suite of on-board sensors performs assigned tasks, which, cumulatively accomplish the assigned mission. Multi-robot teams may be deployed for a wide range of applications like search and rescue [49] [50] [51], emergency response [62], surveillance and reconnaissance [63], as well as convoy support and protection [1] [64]. In such cases, one interesting problem is the 2-D or 3-D strict or loose dynamic formation control problem along with collision avoidance.

In this thesis, the formation control problem is tackled in terms of developing a control algorithm for a multi-robot (or multi-agent) team where each robot/agent interacts with each other and the environment, maintains one or a family of geometric shapes, and avoids collisions. The formation is able to dynamically reconfigure when agents leave or additional agents enter the formation.

## 1.1 Motivation

The motivation of this research stems from the challenge to develop a coordinated control approach to increase multi-robot team capabilities in uncertain environments (addition or departure of agents) while guaranteeing formation scalability and stability. The focus is on the 3-D formation control problem of a team of Unmanned Aerial Vehicles (UAVs) that interact with each other and the environment, and perform a collaborative task, e.g., convoy support. Emphasis is on, primarily, generalizing previously derived 2-D techniques [1] to 3-D, also accounting for collision avoidance, formation reconfiguration and addition or departure of UAVs/agents.

## 1.2 Problem Statement

In this thesis, the 3-D formation control problem ensures that a multi-agent team maintains a formation, while traversing in mission space and avoiding collisions. In order to 'visualize' the 3-D formation, consider a hollow double-surfaced ellipsoid centered at $(x_c, y_c, z_c)$. The objective is to attract all agents to a bounded ellipsoid or ellipsoid-like formation and allow for agents to remain in the formation as they move in 3-D space while avoiding collisions. Agents are attracted to the desired geometric shape using weighted vector fields, accounting for possible formation reconfigurations. It is assumed that the only obstacles present in the mission space are other agents.

## 1.3 Method of Approach

The proposed solution considers (for implementation purposes) the case of protecting an aerial convoy of cargo airplanes by 'surrounding' them with a fleet of UAVs (multi-robot agents) that follow a 3-D geometric shape, defined loosely by dimensions and a

center of mass. Ellipsoid functions are used to create vector fields that control the heading and velocity of individual agents. To attract agents to a bounded ellipsoidal formation, three vector fields are utilized: one attracts agents from points outside the ellipsoid to the bounded area ellipsoid; one pushes agents from points inside the ellipsoid to the bounded area ellipsoid; a third vector field controls collision avoidance and dispersion between agents. The range of influence of these fields is controlled using ramp limiting functions.

## 1.4 Summary of Contributions

The main contribution is the development and verification of a generalized 3-D formation control algorithm using ellipsoidal and ramp functions for controlling multi-agent movement in parallel to dynamic collision avoidance. The formation is able to reconfigure in the event of addition or departure of agents. The proposed methodology is not platform specific and efficiently scales to different team sizes. When compared to other potential field approaches, this method has the advantage of simplicity of vector field generation. Control parameters can be altered to achieve a set of ellipsoid-like formations while other methods are rigid in formation constraints [37]. The avoidance field of each agent is affected only by the number of obstacles/agents present within a certain range, hence, complexity of vector generation does not increase rapidly with addition of obstacles or new agents.

## 1.5 Thesis Outline

The rest of this thesis is organized as follows: Chapter 2 consists of the literature review where the most relevant background information on the behavior, formation control topology and formation control strategies in multi-robot teams are discussed.

Chapter 3 describes the control algorithm used for formation control and provides a theoretical justification. Chapter 4 presents results obtained through software simulations. Chapter 5 consists of concluding remarks and discusses future work.

# Chapter 2

# Literature Review

A robot can be defined, in the most basic sense, as a device consisting of electronic and mechanical units that can be programmed to execute a set of tasks with or without constant human supervision. Robots that can respond to external stimuli and perform certain behaviors that contribute to a desired goal, without human supervision for extended periods of time are called autonomous robots. Majority of today's robots are categorized into one of the following three main types: robotic manipulators [65], mobile robots [1] and humanoids [61]. Mobile robots are further classified into three groups: unmanned ground vehicles (UGVs) [1], unmanned aerial vehicles (UAVs) [2] [5] and unmanned underwater vehicles (UUVs) [66]. The focus of this research is on unmanned aerial vehicles.

Mobile robots find applications in many fields such as land surveying [67], surveillance [63], photography [69], domestic tasks [68], exploration [49] and many more. Mobile robot systems consisting of an individual robot integrated with multiple sensors that is capable of implementing a specific task is called a single-robot system. Figure (2.1) shows examples of single-robot systems. Figure (2.1a) is the Roomba Discovery robotic vacuum cleaner by iRobot. Figure (2.1b) is the Personal Satellite Assistant by

NASA that propels in zero gravity conditions using small fans. It serves as an all-in-one PDA, videophone and air monitor for astronauts. Figure (2.1c) is The Wave Glider by Liquid Robotics which is an ocean monitoring and exploration device. Other well-known single-robot systems include RHINO [38], ASIMO [39], BigDog [41], Mars Rover [40] and NAO [42].

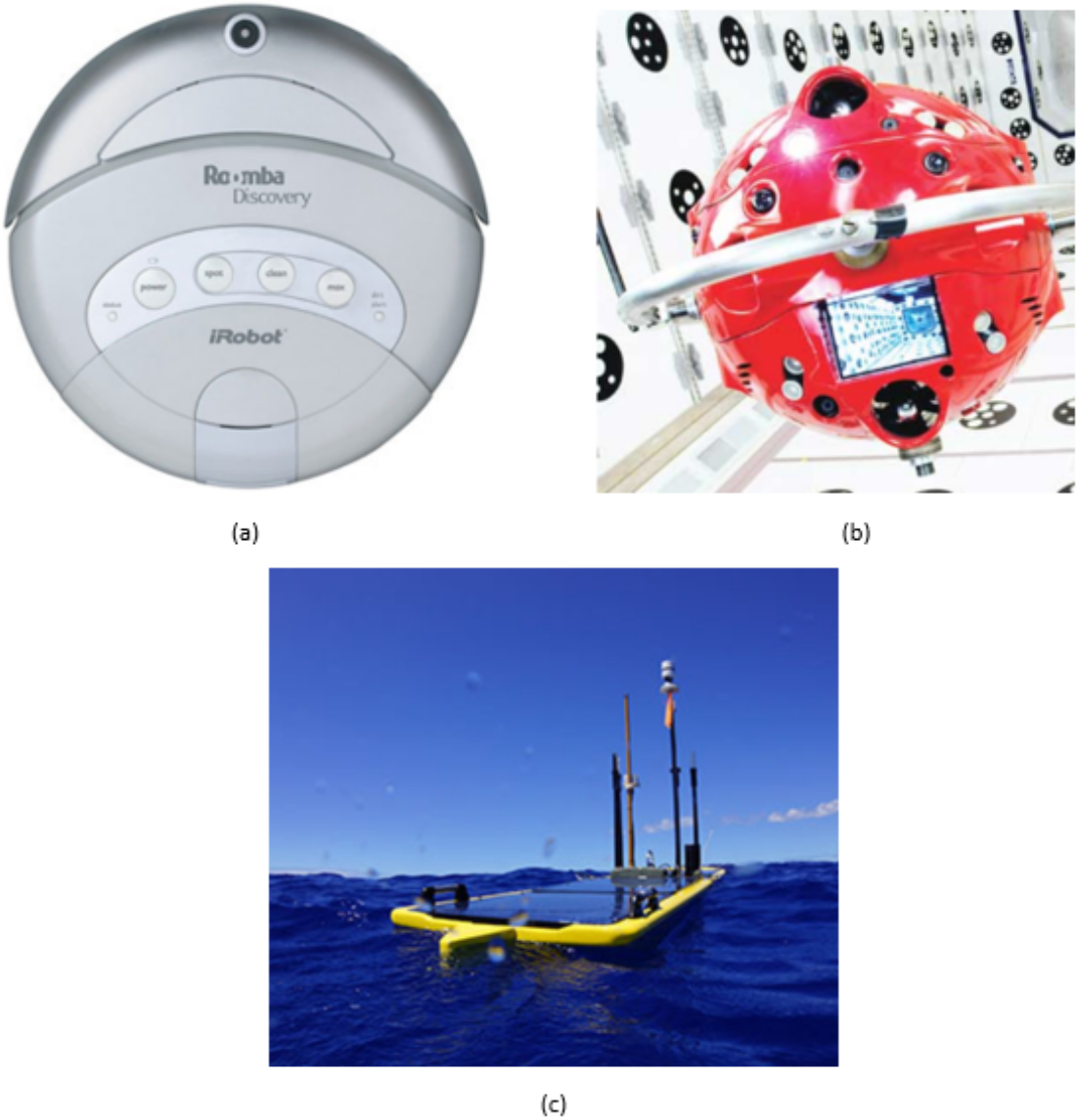


(a) (b)

(c)

Figure 2.1: Examples of single-robot systems: (a) iRobot Roomba Discovery (b) NASA Personal Satellite Assistant [60] (c) Liquid Robotics Wave Glider [59]

Single-robot systems are usually integrated with multiple sensors, thus, requiring advanced component integration mechanism and intelligent control systems. Although major research problems in single robot systems can be resolved efficiently, spatially distributed tasks are inherently impossible for a single-robot system to perform, giving rise to the necessity for multi-robot systems. A robot system comprising of two or more robots is called a multi-robot system. In such systems, individual robots are usually simple in hardware and/or software architecture and interact with each other and the environment to accomplish desired tasks. With respect to their response to external stimulus, behavior of multi-robot system can be classified as shown in Figure (2.2): cooperative and competitive behavior. This research focuses on formation control of a cooperative team of UAVs.

In this chapter, multi-robot behaviors are discussed in Section (2.1), formation control topologies are discussed in Section (2.2) and a comparative study is presented. Section (2.3) discusses various methods or strategies utilized to achieve formation control.

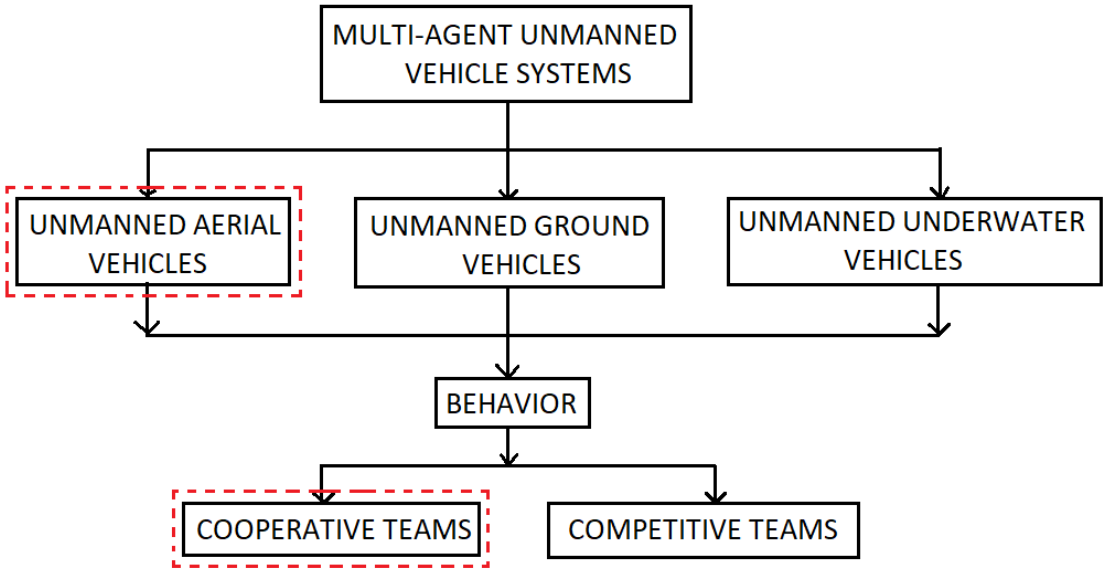


Figure 2.2: Multi-agent unmanned systems and their behavior

## 2.1 Cooperative and Competitive Behavior

The response of a robot to an external stimulus may or may not involve interaction with other robots in the team. Robots which interact with other robots in the team and work towards a common goal are referred to as a team of cooperative robots. Cooperative robots find numerous applications in tasks like exploration, transportation, convoy protection and search and rescue operations. In [3], [43], [54] and [44] cooperative multi-robot teams are used in transportation of objects. Liu et al [46] use a team of cooperative robots to interact with humans and other automated systems to navigate in a laboratory for indoor transportation. Dai et al [47] use a team of cooperative robots to transport a polygonal object by maintaining euclidean distances between each other. In [48], [49], [50], [51] and [45] multi-robot teams perform cooperative foraging tasks. On the contrary, robots which compete against each other to achieve an individual goal or to fulfill their self-interest exhibit competitive behavior. Multi-robot competitive behavior is exhibited in RoboCup [52], a robot soccer league and in robot chess [53].

## 2.2 Formation Control Topologies

The first step to be taken in designing a multi-agent control algorithm is to define the type of control topology to be utilized depending on the communication architecture. Control topologies in autonomous multi-agent teams include: (i) centralized control, where individual agents are controlled by a central control unit (ii) decentralized control, where individual robots rely on local information and local control laws to exhibit a global emergent behavior and (iii) hybrid control.

In centralized control, individual agents receive commands from a central control unit, whereas in decentralized control, communication between team members is unrestricted

and they can share information, to achieve a required mission without the presence of a central agent. Table (2.1) categorizes the formation control topology literature review.

Table 2.1: Formation Control Topologies

| Authors | Year | Formation Representation | Reference Type | Control Topology |
|---|---|---|---|---|
| Desai et al [13] | 2001 | Graph | Directed-edge (leader-follower) | Decentralized |
| Fierro et al [11] | 2001 | Lyapunov candidate functions | Vision based, leader follower | Hybrid |
| Das et al [6] | 2002 | Graph | Directed-edge (leader-follower) | Decentralized |
| Barnes et al [1] | 2009 | Shape functions | Unit-center, neighbor-based | Hybrid |
| Chao et al [14] | 2012 | Formation constraint functions | Nonlinear predictive model, virtual target tracking | Distributed |
| Alejo et al [3] | 2013 | Axis-aligned minimum bounding box | Trajectory-planning, particle swarm optimization | Centralized |
| Rosales et al [2] | 2014 | Null space of Jacobian matrix | Trajectory tracking | Centralized |
| Sanchez et al [4] | 2014 | Offsets from neighbor | Relative neighbors | Decentralized |
| Bereg et al [5] | 2015 | Geometric | Euclidean bipartite matching | Decentralized |
| Ghamry et al [8] | 2015 | Geometric | Trajectory tracking | Decentralized |
| Liu et al [12] | 2015 | Formation constraint functions | Leader follower, adaptive fault control | Centralized |

| | | | | |
|---|---|---|---|---|
| Merrill et al [15] | 2015 | Offsets from neighbor | Mesh networking | Decentralized |
| Seng et al [7] | 2016 | Formation constraints | Potential field, euclidean distance | Distributed |
| Kim et al [9] | 2016 | Formation constraint functions | Target tracking | Decentralized |
| Santana et al [10] | 2016 | Offsets from neighbor | Relative neighbors | Centralized |
| Liang et al [16] | 2016 | Hybrid graphs | Distance-based controllers, virtual target tracking | Hybrid |

### 2.2.1 Centralized Formation Control Topology

In centralized control, there exists a central control unit which commands tasks and plans the motion of all agents which communicate through this unit. Global knowledge about the system, environment and individual robots is available only to the central control unit which is capable of taking optimal decisions for agents and the formation as a whole. However, a centralized system is prone to reduced speeds due to handling large amounts of information and has low tolerance to failure.

In [2], a centralized formation control algorithm handles: (i) shape and orientation control and (ii) centroid control. Shape and orientation control is of higher priority and is placed in the row space of the control matrix and the centroid control is placed in the null space so as to avoid conflict of interest between tasks. With these two objectives, a controller is developed which is capable of achieving multiple-robot control objectives. On the contrary, in this research, the centroid of the formation is broadcasted by a central control unit to all the agents in the formation and orientation is controlled by individual agents.

In [3], the UAVs are required to carry objects from one point to another without colliding with each other. This problem is solved by a centralized control system that constructs two virtual 3D boxes, one around the UAV and the other around the link (connecting object to the UAV) and object. If this area enclosed by the box overlaps with that of another robot, it is considered as a collision. To provide a collision free path, if the axis-aligned 3D bounding boxes overlap, one UAV is made to stay in the same position while the other is made to move towards the goal point. This research uses a similar approach to achieve collision avoidance by creative virtual spheres around members of the team and objects to be avoided.

Santana et al [10] propose a centralized control structure for a heterogeneous leader-follower formation involving a UGV, the leader and a UAV, the follower based on their kinematic models. The leader follower formation controller was derived from the difference between the UAV and the UGV models and the kinematic behavior for the formation is in turn derived. A velocity controller is proposed using pole allocation by state feedback and Kalman filter is used to estimate the feedback information required by the controller. A vision algorithm is used to extract pose data. This research uses potential fields instead of the leader follower approach where the other team members are 'sensed' by each member.

Liu et al [12] propose a centralized method to handle collisions and actuator faults while keeping the formation intact by constructing the leader-follower formation control in the outer loop and the adaptive fault control (AFC) scheme along with collision avoidance in the inner loop. Each UAV is allocated with a virtual repulsive force so as to ensure obstacle avoidance (outer loop). Adaptive control law is implemented in the inner loop to achieve efficient reference tracking. Though obstacle avoidance is not entirely achieved, the algorithm for fault detection is successful. A similar method for obstacle avoidance is used in this research which works successfully.

The advantage of centralized control topology is that the central control agent has global knowledge about the system and can hence coordinate task execution optimally. However, it is efficient only for a small team of robots.

### 2.2.2 Decentralized Formation Control Topology

In decentralized control, inter-agent communication and local control laws operating on individual agents collaborate to achieve a common goal. Sanchez et al [4] design a decentralized leader-follower algorithm that drives individual agents to desired positions relative to other agents and maintains such a position when they carry out missions as a team. Agents are driven to the desired position by means of a distributed trajectory generator and a local nonlinear controller.

In [5], Bereg et al use a decentralized approach to deal with faults in formation of unmanned vehicles (UVs). They propose that when one or more UV is rendered non-functional, reconfiguration can be initiated using computational geometry techniques by re-establishing communication between the remaining UVs, whereas, [15] uses a mesh network for low latency communication between UAVs to ensure easy addition and removal of UAVs. This research uses concept similar to [5] to handle re-configuration in the event of addition or departure of agents.

In [8], Ghamry et al use a Linear Quadratic Regulator (LQR) to control the position of the quadrotor and a sliding mode control (SMC) to control the altitude of the quadrotor. LQR-SMC controllers are implemented for both leader and followers. The dynamic model of the quadrotor is divided in to two subsystems - a fully-actuated subsystem and an under-actuated subsystem. The fully-actuated subsystem is used to design altitude and heading controller, and the under-actuated subsystem is used to control translational dynamics to achieve the required position. Decentralized control topology is used.

Seng et al [7] propose a distributed decentralized control method for formation control of non-holonomic ground vehicles. The robot closest to a predefined destination is assigned as local leader and other robots are assigned formation positions sequentially. Velocity controller and angular velocity controllers are used to reduce the distance between robots and the assigned formation position, thereby reducing the Euclidean distance error. Only local information is required to calculate cost rather than utilizing global coordinates. Obstacle avoidance is implemented using potential fields. This research achieves formation control without pre-defining the desired position of agents.

Kim et al [9] build a controller for a multiple UAV system such that each agent moves individually to positions from which they can gather maximum information about the target. The condition for the system to converge to a given set of critical points and for the navigation function to minimize at the critical points is deduced. The results proved in this paper are confined to a specific case of an 8-rotary wing unmanned aircraft and a target in 2-D space only. On the contrary, this research is not platform dependent and does not use target information for motion planning.

In [13], a framework for modeling a formation of mobile robots using graph theory is presented and changes in formation are related to changes in graph structure. A decentralized feedback controller compatible with a readily available higher level motion planner is proposed. As a result, groups change into a different formation to avoid obstacles and then merge again to the original formation. This research uses potential fields to avoid obstacles and achieve a desired geometric formation.

Chao et al [14] use a distributed nonlinear model predictive control to track virtual points that determine the formation shape. Cost penalty is introduced to achieve obstacle and inter-vehicle collision avoidance. Additionally, a priority strategy is proposed for inter-vehicle collision avoidance. This research does not implement target tracking, instead agents are attracted towards a potential trench in the mission space.

In decentralized control topology, computational efforts are distributed and individual robots are autonomous in decision making. Unlike centralized control, this topology is scalable, robust and adaptable to environmental changes, has fewer communication requirements and has greater potential in real-time applications.

### 2.2.3 Hybrid Formation Control Topology

Majority of formation control approaches use hybrid control topology, a combination of centralized and decentralized control topology, as traditional control theory may fail in situations where the control problem consists of several sub-tasks.

Fierro et al [11] describe a trajectory for non-holonomic robots while maintaining a desired formation by using the leader-follower approach. This problem is approached by designing a set of controllers for each robot such that the team of robots can switch from an initial formation to a desired formation. Three controllers are defined, two of which are described in [19]. The third controller for obstacle detection is described in this paper where a virtual robot is defined to follow along the wall of the obstacle. In this research, switching from one formation to another can be achieved by changing control parameters, eliminating the necessity to develop a separate algorithm.

Similar to [13], Liang et al [16] use graph structure for formation control where hybrid graphs are stabilized by distance-based controllers. Barnes et al [1] use hybrid architecture where a combination of normal and sigmoid functions generate artificial potential fields to attract the agents to a required geometric shape in the work space.

The formation control methodology presented in this research uses a hybrid control topology. The centroid of the aerial convoy to be protected is broadcast in the team and the task of surrounding the convoy in a geometric shape, avoiding collisions and maneuvering in the mission space are performed using local information.

## 2.3 Formation Control Strategies

Formation control in multi-robot teams has been extensively studied and three main formation control strategies have been identified: (i) leader-follower and graph theory based (ii) behavior-based and potential fields and (iii) virtual structure. Figure (2.3) states the different types of formation control topologies and formation control strategies. Behavior-based and potential field strategy is decentralized in nature and virtual structure strategy is centralized in nature. This thesis uses potential field based formation control strategy to achieve formation control in a team of cooperative UAVs.

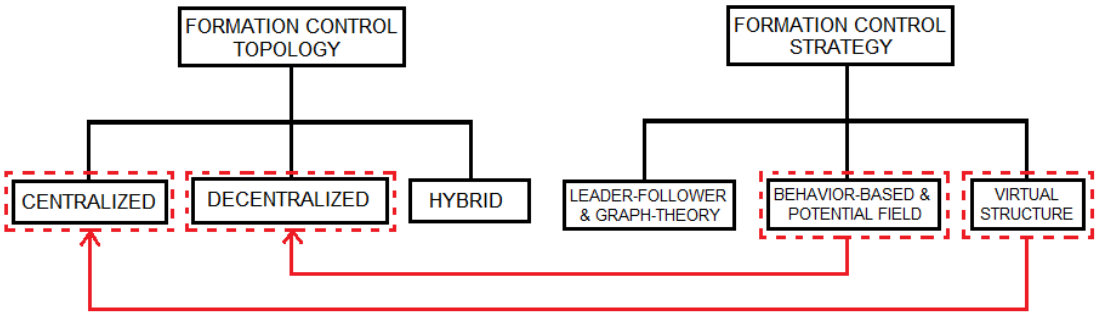


Figure 2.3: Types of formation control topologies and strategies

Formation control strategies use various shapes of formations depending on the scenario or task to be executed. Formation shapes may be a line, circle/sphere, ellipse/ellipsoid or polygon. Table (2.2) shows a list of formation control strategies that have been reviewed.

Table 2.2: Formation Control Strategies

| Authors | Year | Formation Representation | Formations | Formation Control Topology |
|---|---|---|---|---|
| Desai et al [19] | 1998 | Directed Graphs | Line, triangle | Leader-follower |

| | | | | |
|---|---|---|---|---|
| Fierro et al [11] | 2001 | Vision-based size and location | Triangle, rectangle, line | Leader-follower |
| Desai et al [13] | 2001 | Directed graphs | Line, triangle, rectangle | Leader-follower |
| Tabuada et al [20] | 2005 | Inter-agent constraints using graphs | Line, triangle, diagonal | Leader-follower |
| Ren et al [57] | 2007 | Distance constraints w.r.t a virtual point of reference | Square, rectangle | Virtual structure |
| Paul et al [21] | 2008 | Inter-agent distances | Triangle, line (fixed altitude) | Virtual leader, potential field |
| Barnes et al [1] | 2009 | Shape function | 2D line, wedge, ellipse, circle | Potential field |
| Bunic et al [23] | 2012 | Potential field trenches at desired target locations | Wedge (fixed altitude) | Potential field |
| Deng et al [25] | 2013 | Inter-agent constraints | Not specified | Consensus algorithm |
| Ahmad et al [31] | 2013 | Color histogram matching using probability density function | Application specific | Particle filter based algorithm |
| Benzerrouk et al [56] | 2014 | Agent-target distance and agent kinematic constraints | Triangle | Virtual structure |
| Nielsen et al [17] | 2015 | Vision-based size and location | Line, triangle | Leader-follower |
| Lima et al [28] | 2015 | Agent-target distance constraint | Not specified | Minimizing cost function |

| | | | | |
|---|---|---|---|---|
| Bereg et al [5] | 2015 | Inter-agent distances | Line, diamond, arc, circle in 3D, hemisphere | Geometric approach |
| Whitzer et al [18] | 2016 | Reference tracking by B-spline fitting | Line, column, diagonal, diamond, triangle | Leader-follower |
| Santana et al [10] | 2016 | Vision-based size and location | Not specified | Leader-follower |
| Braga et al [27] | 2017 | Agent-target distance constraint | 3D line, column, triangle | Virtual structure, leader-follower, behavior-based |
| Roy et al [55] | 2018 | Formation pattern preserved inside a virtual structure | 2D Triangle, ellipse, star | Virtual structure |

### 2.3.1 Leader-Follower and Graph Theory Based Formation Control Strategies

In leader-follower strategy, one member of the multi-robot team is assigned as the "leader" and other members of the team, called as "followers" are made to track the position and orientation of the leader by maintaining an offset. In [4], [8], [12], [17], [10], [19], [20] use leader-follower approach to achieve formation control. [10], [11], [17] and [18] use a camera to identify the position of the leader and the followers are made to remain at a certain position and possess a specified dimensions in the camera view in order to achieve a formation. The followers are not required to have information about the position and orientation of the leader.

In [4], a leader follower coordination scheme with two quadrotors is presented. The distance from the leader to the followers is specified by a set of inter-agent distances. Similar to [18], each agent maintains its desired position relative to the reference trajectory instead of the complete position and orientation of the leader. They consider for coordination only the spacial position of the quadrotor. In this research, no 'leader' is assigned in the team. Agents are attracted to a potential trench in the mission space.

Nielsen et al [17] propose a Lyapunov based approach for vision based formation control using leader-follower method. Formation control of quadrotors using only camera measurements is achieved by keeping the quadrotor being followed at a fixed size and location in the camera's view. This research utilized potential field vectors for formation control.

Santana et al [10] use leader-follower approach to achieve formation control of a heterogeneous system. Vision algorithm is used to extract pose data. The leader follower formation controller was derived from the difference between the UAV and the UGV models and the kinematic behaviour of the formation is in turn derived. The approach presented in this research is however, independent of the platform used.

In [11], a trajectory for nonholonomic robots to maintain a desired formation using leader-follower approach is described. A controller for obstacle detection is described where a virtual robot is defined to follow along a wall. There is no communication between leader and follower. A vision system provides the range and angle of the observed leader which is used by the velocity controller for formation control. This research uses potential fields to generate velocity vector for each team member.

In [19], formations represented by directed graphs are controlled using a method of feedback linearization control utilizing only local sensor based information. Two scenarios are presented. In the first scenario, one robot follows another by controlling the relative distance and orientation between the two. In the second scenario, one robot

maintains its position in the formation by maintaining a specified distance from two robots, or from one robot and an obstacle in the environment. Desai et al [13] use a similar approach based on graph theory to achieve transition from one formation to another. In the presented research, inter-agent collisions are avoided by defining a repulsive vector field around each agent and change in formation shape is achieved by altering control parameters.

Tabuada et al [20] model individual agent kinematics and inter-agent constraints using formation graphs. They construct a model of the formation as a whole guaranteeing that the formation constraints are preserved along any of its trajectories. Hence, a lower dimension control is proven to maintain the same constraints. This is well suited for higher levels of control as it allows the formation to be considered as a single entity. However, in this research potential fields are used to define inter-agent constraints

In leader follower method, each robot in the team directly or indirectly depends on the leader. Failure of the leader requires reassigning a new leader and re-initiate the flow of information which can be computationally expensive and difficult.

### 2.3.2 Behavior-Based and Potential Field Based Formation Control Strategies

Behavior-based control systems decompose the main formation control task into sub-tasks that are to be performed by each member of the team. The task of each member is weighed based on their importance and contribution to the main task. The basic concept of potential field method consists of filling the robot work space with artificial potential fields, in which the robots are attracted to their respective desired positions [22]. The desired positions are regions of minimal potential energy, that is, a potential trench. Robots are is pushed away from the obstacles using a repulsive potential field. Often, a

combination of behavior-based control and potential field based control are combined for multi-robot formation control. Some studies like [21], [7] use a combination of potential field based control and other strategies like leader-follower and graph theory to achieve formation control, where, potential field based control is used for obstacle and collision avoidance.

Barnes et al [1] use bivariate normal functions to generate artificial potential fields which are utilized for formation control of a swarm of ground robots. Sigmoid limiting functions are used to tightly confine the swarm to an elliptical path. A perpendicular vector field is added to this narrow elliptical band to control the direction of the swarm. The control parameters in this function determine the range of influence of the avoidance vector. A similar approach is presented in this thesis for robots in 3-D space where elliptical and ramp functions are used to generate vector fields to attract robots to a bounded geometric shape.

Paul et al [21] use virtual leader approach for formation control for a team of helicopters. They use the potential field approach for collision and obstacle avoidance. This method is however, is limited to only VTOL UAVs. Similarly, [7] uses potential field method for obstacle avoidance and introduces formation morphing as a fail-safe solution should formation scaling fail to maintain the formation structure. Similarly, this research uses potential fields to achieve obstacle avoidance.

In [23], formation control is achieved by target tracking using a potential function which is a Gaussian function weighted by the modulus of vector differences. Agent-target and inter-agent vector differences weights to the potential function and the sum of the two is the force on the agent. Each agent moves towards a potential trench which is the target. Control parameter dependent singularity is eliminated and control parameter independent singularity exists. Similarly, in this research, agents move towards a potential trench but the positions of the target are not specified.

Behavior-based approach is highly decentralized in topology and is strongly dependent on local inter-agent information. However, this strategy does not produce a precise geometric formation.

### 2.3.3 Virtual Structure Formation Control Strategies

Tan et al [58] were pioneers in the concept of virtual structures. Braga et al [27] combine virtual structure, leader follower and behavior based methods to achieve formation control of UAVs. Virtual structure method is used to assign a problem for each UAV in the formation and the UAVs use leader follower and behavior based control to achieve formation. In [55], a circular virtual structure encloses the multi-robot team and the team approaches the target by preserving a pattern inside this virtual structure. Obstacles are avoided by shrinking the size or altering the shape of the virtual structure. Inter-agent formation constraints are made flexible using a spanning-tree-assisted-shape-matching algorithm to accommodate the change in dimensions of the virtual structure.

In [56], a set of virtual dynamic target points are generated by a controller. The controller generates linear and angular velocities for each robot based on its kinematic constraints such that they are attracted towards a dynamic target while simultaneously avoiding obstacles. Obstacles avoidance is achieved using limit cycle method. In this research, agent positions are defined with respect to the formation center and the entire formation moves as the center moves. A similar approach is seen in Ren et al [57], where a virtual coordinate frame with a virtual center as a point of reference such that the desired states of all the robots in the team are defined with respect to this virtual coordinate frame. Hence, motion planning for the entire team is achieved by simply defining the motion planning algorithm for the virtual center to track a desired set of waypoints which ensures that the formation is preserved.

In cases when a precise geometric formation is required, the virtual structure strategy is used. Unlike in potential field based control, the formation structure obtained in virtual structure strategy is very precise and tight. However, this strategy is centralized in nature due to which these systems are less robust to failure.

### 2.3.4 Other Formation Control Strategies

Many other formation control strategies exist, which do not fit in the previously described categories. Alejo et al [3] use Particle Swarm Optimization to provide a collision-free 4D trajectory planning for UAVs carrying objects. This method however, increases the overall time taken to achieve the goal and is not the optimum method.

Bereg et al [5] use a geometric approach to deal with faults in a formation of Unmanned Vehicles (UVs). It proposes that when one or more UVs in a formation is rendered non-functional, formation re-configuration can be initiated with the remaining UVs. Each UV has a range within which reliable communication is limited to and another minimum range for collision avoidance. Two UVs can communicate only when their minimum communication ranges intersect. A similar constraint is defined in this thesis to achieve collision avoidance between agents.

Deng [25] and Rezaei [26] propose a consensus algorithm to achieve formation control. [25] requires only speed, heading angle and height to be communicated from neighbor-to-neighbor. This method is robust, scalable, requires less communication between members and hence makes this easy to implement. In [26], Razaei et al propose an observer-based consensus algorithm to deal with unknown disturbances in multi-agent systems for distributed leaderless and leader-follower of multi-agent systems consisting of agents having linear dynamics.

Franchi et al [24] describe a method of formation control using only relative angles. A formation controller is designed based on only bearing measurements. In this research, the orientation of each agent is determined by the resultant normalized vector field acting on it at any instant of time. Lima et al [28] propose a formation control strategy to minimize the uncertainty about object tracking by including the uncertainty as a cost function that is to be minimized. The target estimator is based on particle filters.

Zarzhitsky et al [29] designed and developed a method to combine the data received by sensors on all UAVs using Kalman filtering to achieve a group of UAVs to search, detect and locate stationary ground targets. This results in an increased efficiency of target estimation. In [30], a fuzzy logic controller is used for formation control and a non-linear State-Dependent Riccati Equation (SDRE) is used for flight control. Both these controllers do not require linearization or gain scheduling. Ahmad et al [31] propose a sensor fusion algorithm for 3D object tracking that is particle-filter based. This method is based on color histogram matching of the object which is a solution for a hindered or partially hindered object. Each robot has a "confidence factor" for observing and estimating the position of the target. This factor is parameterized as a probability density function.

## 2.4 Summary

This chapter presents a survey on behavior of robots, decision-making mechanisms and strategies of formation control in multi-robot teams. It is evident that, based on the goal or task of the mission, one mechanism or strategy might be better than the other. In this work, UAVs exhibit cooperative behavior. In terms of decision-making mechanisms or formation control topologies, the proposed methodology uses hybrid topology. The

position of the asset to be protected and the size of the formation is broadcasted in the group and obstacles/other UAVs are either locally sensed or their position information can be broadcasted in the group.

This work uses potential field based formation control strategy to attract the UAVs to the desired formation shape. Although virtual structure strategy provides a more precise geometric formation, a tighter formation can be achieved in the potential field approach by varying the formation control parameters. In the proposed methodology, the formation is able to dynamically re-configure on the event of departure or addition of UAVs. Unlike the approach is [23], the proposed methodology does not use potential fields to attract UAVs to predefined target points. Instead, UAVs are made to disperse in potential field contours giving rise to the possibility of a number ellipsoid-like formations.

# Chapter 3

# Formation Control Approach

The objective of this work is to attain a single or a set of loose formations by attracting UAVs to a desired bounded ellipsoid or ellipsoid-like shape in 3-dimensional space. This is achieved by defining a vector using ellipsoidal functions to create potential peaks and trenches in the mission space. UAVs traverse in the direction of steepest descent. Vector fields are defined such that they (i) attract UAVs located outside the desired ellipsoid towards the bounded ellipsoid area and (ii) push UAVs located inside the ellipsoid away from the center, towards the bounded ellipsoid area. The surface of the ellipsoid is at a low potential field with increasing potential fields inside and outside the ellipsoid. Another vector field is defined to ensure collision avoidance and dispersion of UAVs. Each of these vector fields are required to diminish to zero after a certain range so that the agents hit a global minimum on reaching a required point in the formation. Ramp functions are utilized to limit these vector fields appropriately. UAVs belonging to the team are considered to be identical in capabilities.

## 3.1 Description of Ellipsoidal Formation Function

At every instant of time the UAVs/agents can be visualized as particles, moving in an artificial potential field derived from the ellipsoid function:

$$f(x, y, z) = (x - x_c)^2 + \gamma(y - y_c)^2 + \lambda(z - z_c)^2 \tag{3.1}$$

where $(x, y, z)$ is the current agent position and $(x_c, y_c, z_c)$ is the center of the ellipsoid function in (3.1) with respect to the world reference frame. $\gamma$ is the ratio of semi principal x-axis to the semi principal y-axis and $\lambda$ is the ratio of the semi principal x-axis to the semi principal z-axis of the ellipsoid. By changing the ratios $\gamma$ and $\lambda$ eccentricity of the ellipsoid can be altered. The x, y and z partial derivatives of Equation (3.1) create vector fields that provide heading and velocity of agents as follows:

$$d_x = 2(x - x_c) \tag{3.2}$$

$$d_y = 2\gamma(y - y_c) \tag{3.3}$$

$$d_z = 2\lambda(z - z_c) \tag{3.4}$$

Equations (3.2), (3.3) and (3.4) together generate vector fields $(d_x, d_y, d_z)$ and $(-d_x, -d_y, -d_z)$ in 3-dimensional space as shown in Figures (3.2) and (3.3) respectively. These vector fields are explained in detail in Section (3.3.1).

## 3.2 Description of Formation Problem

In order to describe the formation control problem, it is discussed in reference to convoy protection of aerial cargo planes by 'surrounding' them with a fleet of UAVs in

some geometric shape. With the position of the convoy vehicles known, the centroid of the convoy $(x_c, y_c, z_c)$ is taken as center of the function in Equation (3.1). Concentric ellipsoids are defined with center $(x_c, y_c, z_c)$ and dimensions, based on convoy size. A control algorithm needs to be designed to attract agents to the region between these ellipsoids resulting in a loose geometric shape. Attractive and repulsive fields, and position and velocity vectors of individual agents are calculated relative to $(x_c, y_c, z_c)$ which serves as the origin of the local reference frame.

Formation is achieved by attracting members of the team to the ellipsoid which is described as a set of points $(x, y, z) \in R^3$ satisfying:

$$R^{*2} = (x - x_c)^2 + \gamma(y - y_c)^2 + \lambda(z - z_c)^2 \tag{3.5}$$

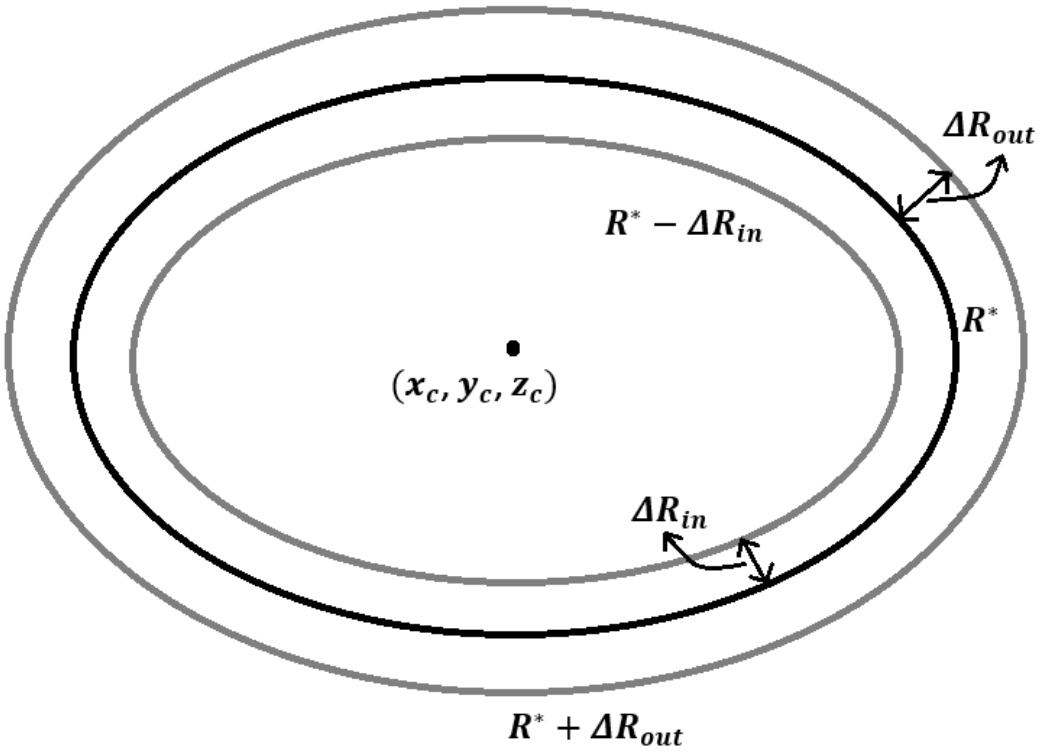


Figure 3.1: Ellipsoidal band cross-section

If $R^*$ is the radius of the required ellipsoid, the goal is to achieve a loose formation by creating a region around $R^*$ bounded by an outer ellipsoid with radius $R_{out}$ and an inner ellipsoid with radius $R_{in}$. The agents are attracted to and "trapped" in this $R^*$ neighborhood. Within these boundaries, agents have considerable freedom of movement subject to collision avoidance. Figure (3.1) describes the bounded $R^*$ region. Assuming $\triangle R_{out} = \triangle R_{in}$, the outer and inner boundaries, $R_{out}$ and $R_{in}$ are given by:

$$R_{out} = R^* + \triangle R_{out} \tag{3.6}$$

$$R_{in} = R^* - \triangle R_{in} \tag{3.7}$$

Constructing the vector field using the normalized gradient from Equations (3.2, 3.3, 3.4), for every agent $(x_i, y_i, z_i)$ let the gradient field vector have the form [1]:

$$V_i(x_i, y_i, z_i) = \begin{cases} W_i(x_i, y_i, z_i) \frac{1}{L(x_i, y_i, z_i)} \begin{pmatrix} (x_i - x_c) \\ \gamma(y_i - y_c) \\ \lambda(z_i - z_c) \end{pmatrix}, & \text{for } (x_i, y_i, z_i) \neq (x_c, y_c, z_c) \\ \begin{pmatrix} 0 \\ 0 \\ 0 \end{pmatrix}, & \text{for } (x_i, y_i, z_i) = (x_c, y_c, z_c) \end{cases} \tag{3.8}$$

where,

$L(x_i, y_i, z_i) = \sqrt{(x_i - x_c)^2 + \gamma^2(y_i - y_c)^2 + \lambda^2(z_i - z_c)^2}$

$\frac{1}{L(x_i, y_i, z_i)} \begin{pmatrix} (x_i - x_c) \\ \gamma(y_i - y_c) \\ \lambda(z_i - z_c) \end{pmatrix}$ is a unit vector which gives heading to agent "i" and has unit magnitude. Note that the unit vector points away from the center of the ellipsoid for

any $(x_i, y_i, z_i)$. $W_i(x_i, y_i, z_i)$ is the sum of magnitudes of all vectors acting on the "i"th agent (described in Section (3.3.2)). In the defined vector field, agents starting within the $R^* - \triangle R_{in}$ ellipsoid where:

$$R^* = \sqrt{(x_i - x_c)^2 + \gamma^2(y_i - y_c)^2 + \lambda^2(z_i - z_c)^2} \tag{3.9}$$

move away from the center until they reach the $R^*$ neighborhood. Agents starting outside the $R^* + \triangle R_{out}$ ellipsoid move towards the center until they reach the $R^*$ neighborhood. Eventually, all agents are trapped within the $R^*$ neighborhood bounded by:

$$(R^* - \triangle R_{in}) \leq R \leq (R^* + \triangle R_{out}) \tag{3.10}$$

resulting in a loose ellipsoidal formation.

## 3.3 Description of Vector Fields and Limiting Functions

### 3.3.1 Attractive and Repulsive Vector Fields

In order to hold the agents in the $R^*$ neighborhood, two vector fields are required: one to attract the agents that lie outside the $R^*$ band towards the bounded ellipsoidal region and the other to push agents lying inside the $R^*$ band away from the center. These two fields are defined using the gradient vector fields described in Section (3.1). $G^+ = (d_x, d_y, d_z)$ is directed away from the center of formation as shown in Figure (3.3) and $G^- = (-d_x, -d_y, -d_z)$ is directed towards the bounded ellipsoid region from outside and is shown in Figure (3.2).

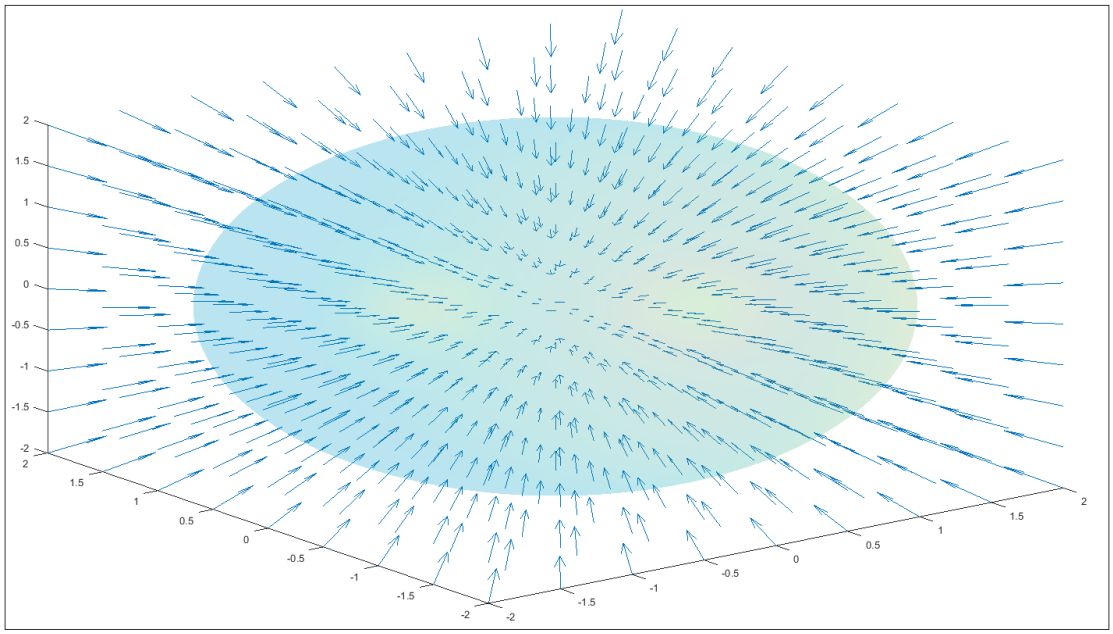

Figure 3.2: Vector field directed towards the center of ellipsoid ($G^-$)

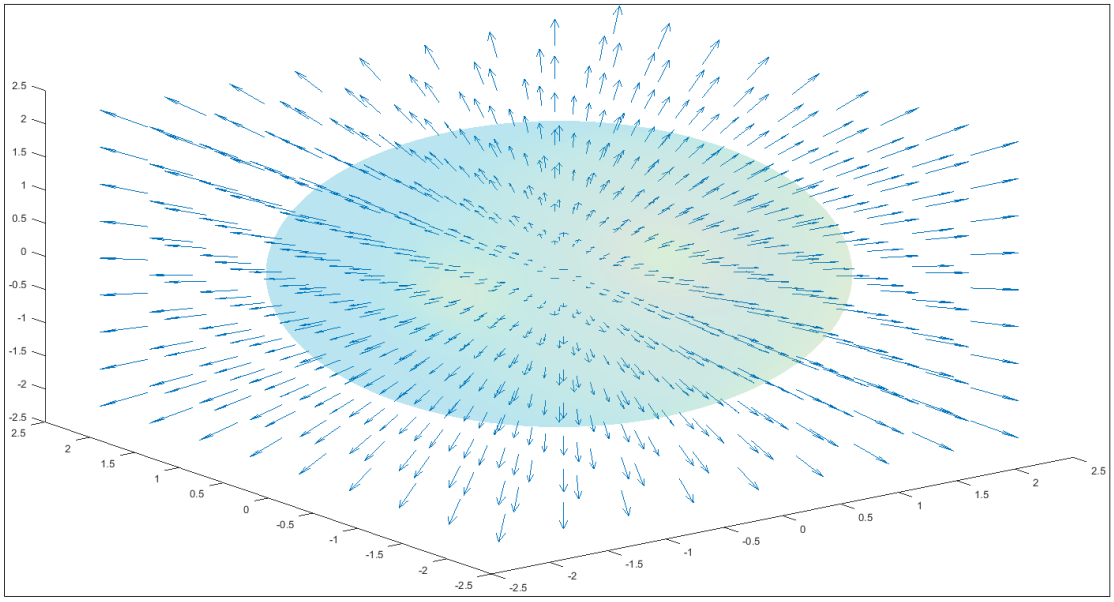

Figure 3.3: Vector field directed away from the center of ellipsoid ($G^+$)

### 3.3.2 Limiting Functions for Attractive and Repulsive Fields

The influence of $G^+$ and $G^-$ gradient field vectors are restricted to the $R^*$ neighborhood by multiplying with limiting functions. In this case, ramp functions are used to limit the influence of $G^+$ to $R^* - \triangle R_{in}$ ellipsoid and $G^-$ to $R^* + \triangle R_{out}$ ellipsoid. Therefore, agents lying outside the $R^*$ region experience only attractive field while those lying inside experience only repulsive field. Agents within the $R^*$ neighborhood (as described in Equation (3.10)), experience neither attractive nor repulsive fields. The general case of a ramp function is as in Figure (3.4).

$$r(t) = \begin{cases} tu(t), & \text{if } t > 0 \\ 0, & \text{otherwise} \end{cases} \tag{3.11}$$

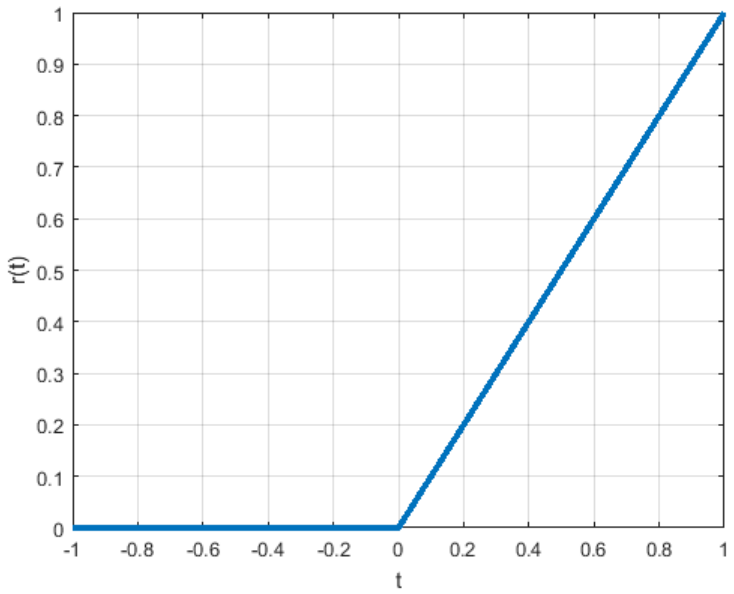


Figure 3.4: General ramp function

The $G^-$ vector field (directed towards the formation center) requires a limiting function which decreases as the distance from the center approaches $R^* + \triangle R_{out}$, such a limiting function is given by:

$$S^-(r, R_{out}, R^*) = \begin{cases} \frac{(r-R_{out})}{R^*}, & \text{if } r > R_{out} \\ 0, & \text{otherwise} \end{cases} \tag{3.12}$$

The $G^+$ vector field (directed away from the formation center) requires a limiting function which decreases as the distance from the center approaches $R^* - \triangle R_{in}$, such a limiting function is given by:

$$S^+(r, R_{in}, R^*) = \begin{cases} \frac{-(r-R_{in})}{R^*}, & \text{if } r < R_{in} \\ 0, & \text{otherwise} \end{cases} \tag{3.13}$$

Where $r = \sqrt{(x-x_c)^2 + \gamma^2(y-y_c)^2 + \lambda^2(z-z_c)^2}$ is the weighted distance of the agent $(x, y, z)$ from center of formation and is never negative. The $G^+$ field, limited by $S^+$ diminishes to zero at $R^* - \triangle R_{in}$ and the $G^-$ field, limited by $S^-$ diminishes to zero at $R^* + \triangle R_{out}$. Therefore, from Equation (3.8), $W_i(x_i, y_i, z_i)$ can be written as:

$$W_i(x_i, y_i, z_i) = S^+(x_i, y_i, z_i) - S^-(x_i, y_i, z_i) \tag{3.14}$$

Since $r = \sqrt{(x_i-x_c)^2 + \gamma^2(y_i-y_c)^2 + \lambda^2(z_i-z_c)^2}$ and $S^+$ and $S^-$ are functions of the weighted distance, $W_i(x_i, y_i, z_i)$ becomes:

$$W_i(r) = S^+(r) - S^-(r) \tag{3.15}$$

Figure (3.5) shows the variation in magnitude of $S^{+}(r)$ and $S^{-}(r)$ limiting functions with weighted distance 'r' from the center of formation, where $R^{*} = 75$ units, $R_{in} = 70$ units, $R_{out} = 80$ units.

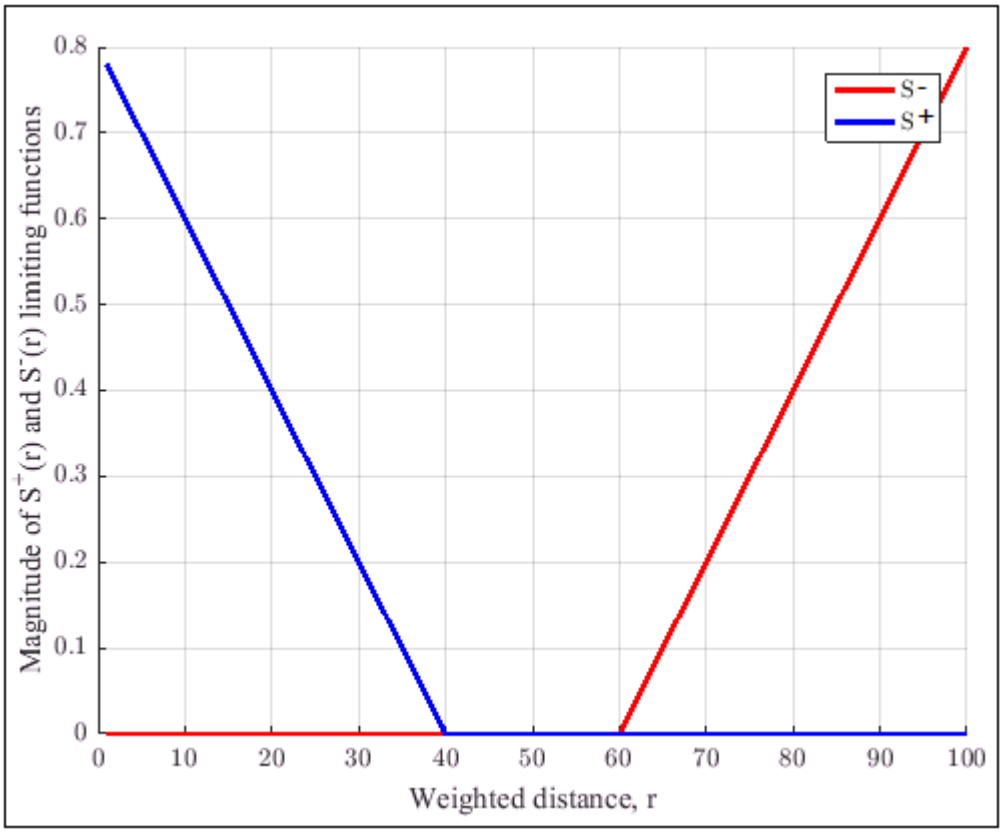


Figure 3.5: $S^{+}(r)$ and $S^{-}(r)$ limiting functions

When combined, normalized gradient field vectors $G^{+}$ and $G^{-}$ with their respective limiting functions from Equations (3.12) and (3.13) provide the velocity vector for individual agents with reference to the center of formation:

$$\begin{pmatrix} v_{xi} \\ v_{yi} \\ v_{zi} \end{pmatrix} = (S^{+} - S^{-}) \frac{1}{\sqrt{d_{xi}^{2} + d_{yi}^{2} + d_{zi}^{2}}} \begin{pmatrix} d_{xi} \\ d_{yi} \\ d_{zi} \end{pmatrix} \tag{3.16}$$

### 3.3.3 Collision Avoidance and Agent Dispersion Fields

In addition to attracting agents to the $R^*$ neighborhood, another necessary aspect is collision avoidance and dispersion of agents within the $R^*$ band. The same concept of potential fields is used and a third gradient vector field is defined. While agents maintain a particular formation, additional restrictions are imposed on them in terms of minimum and maximum allowable inter-agent distances. It is assumed that the only obstacles in mission space are other agents. Minimum distance defined between agents is for collision avoidance whereas, maximum distance defined is to achieve dispersion of agents within the $R^*$ band.

Assume each agent to be surrounded by a virtual sphere of as shown in Figure (3.6), the overlap of which results in collision. The minimum distance between any two agents is $\triangle R_{avoid}$. The radius of this virtual sphere can be increased to $R_{spacing}$ to achieve dispersion of agents within the $R^*$ band. With each agent located at the center of the virtual sphere, collision avoidance is achieved by defining a gradient vector field directed away from the agent, similar to the $G^-$ field. While entering this sphere of another agent, the current agent experiences maximum repulsive force. Any agent lying outside the $R_{spacing}$ sphere does not experience any repulsive field.

Gradient vector field directed away from the center of mass of each agent is given by:

$$\begin{pmatrix} d_{x_{avoid}} \\ d_{y_{avoid}} \\ d_{z_{avoid}} \end{pmatrix} = \begin{pmatrix} 2(x - x_{co}) \\ 2(y - y_{co}) \\ 2(z - z_{co}) \end{pmatrix} \tag{3.17}$$

Where, $(x_{co}, y_{co}, z_{co})$ is the other agent's location. The vector field in Equation (3.17) has a positive sign, this is because the corresponding normalized vector is always pointing away from $(x, y, z)$.

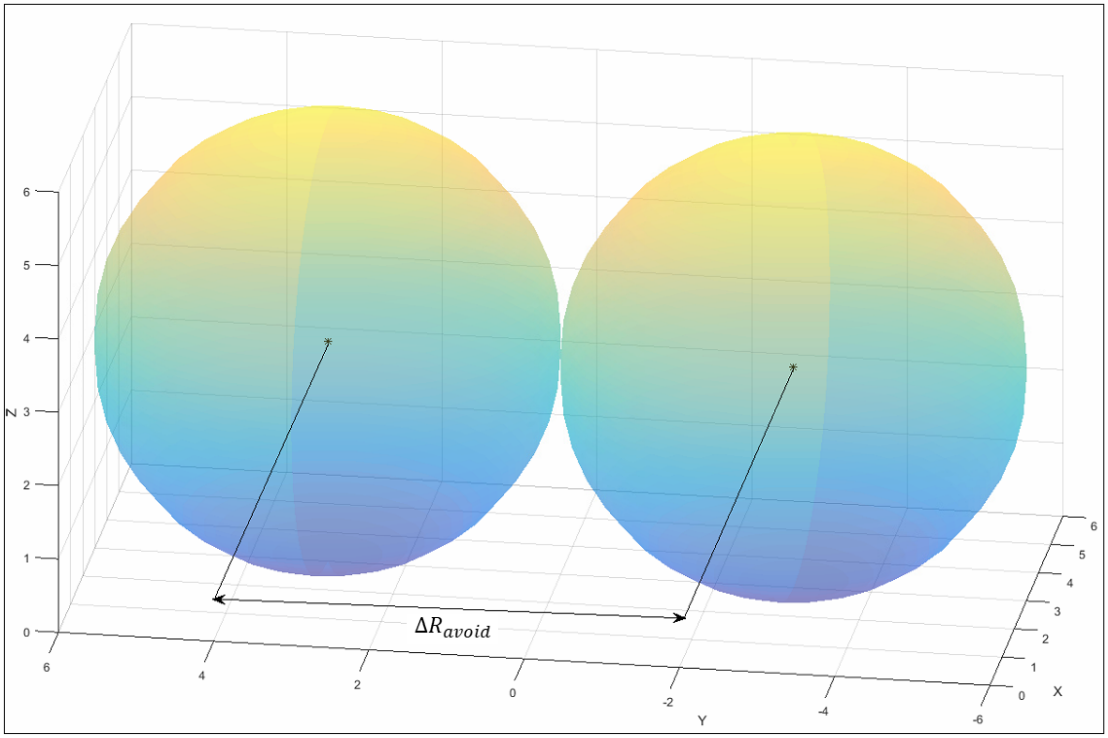


Figure 3.6: Minimum distance between any two agents

The gradient vector field in Equation (3.17) is limited using a ramp limiting function which is defined as:

$$S_{avoid}(r_{co}, \triangle R_{avoid}, R_{spacing}) = \begin{cases} \frac{2\triangle R_{avoid} - r_{co}}{\triangle R_{avoid}}, & \text{if } r_{co} < \triangle R_{avoid} \\ \frac{R_{spacing} - r_{co}}{R_{spacing}}, & \text{if } \triangle R_{avoid} \leq r_{co} < R_{spacing} \\ 0, & \text{otherwise} \end{cases} \quad (3.18)$$

Where, $r_{co} = \sqrt{(x - x_{co})^2 + (y - y_{co})^2 + (z - z_{co})^2}$ which is the distance between the current agent $(x, y, z)$ and another agent $(x_{co}, y_{co}, z_{co})$.

Therefore, the velocity vector which provides velocity and heading for each agent $(x_i, y_i, z_i)$ to be attracted to the desired ellipsoidal formation is:

$$\begin{pmatrix} v_{xi} \\ v_{yi} \\ v_{zi} \end{pmatrix} = (S^+ - S^-)\frac{1}{\sqrt{d_{xi}^2 + d_{yi}^2 + d_{zi}^2}} \begin{pmatrix} d_{xi} \\ d_{yi} \\ d_{zi} \end{pmatrix} + \sum_{j=1}^{N-1} S_{avoid_j} \frac{1}{\sqrt{d_{x_{avoid_j}}^2 + d_{y_{avoid_j}}^2 + d_{z_{avoid_j}}^2}} \begin{pmatrix} d_{x_{avoid_j}} \\ d_{y_{avoid_j}} \\ d_{z_{avoid_j}} \end{pmatrix} \tag{3.19}$$

The above equation results in a static formation of 'N' agents. The design can be scaled to different team sizes by altering the dimensions of the formation ($R^*$, $\triangle R_{out}$ and $\triangle R_{in}$), to accommodate additional agents. It can be observed that the velocity expression for each agent is relative to the center of the formation. Hence, shifting the center of formation from one waypoint to another results in a dynamic formation with collision avoidance. If the maximum velocity of each agent is '$V_{max}$' units, the velocity expression in Equation (3.19) is limited by the condition:

$$V_i(x_i, y_i, z_i) = \begin{cases} \begin{pmatrix} v_{xi} \\ v_{yi} \\ v_{zi} \end{pmatrix}, & \text{if } |V_i(x_i, y_i, z_i)| \leq V_{max} \\ V_{max}, & \text{if } |V_i(x_i, y_i, z_i)| > V_{max} \end{cases} \tag{3.20}$$

Where, $|V_i(x_i, y_i, z_i)| = \sqrt{v_{xi}^2 + v_{yi}^2 + v_{zi}^2}$ and $\begin{pmatrix} v_{xi} \\ v_{yi} \\ v_{zi} \end{pmatrix}$ is given in Equation (3.19).

## 3.4 Justification for Convergence of Agents in $R^*$ region

Recall Equation (3.15), $W(r)$ can be written as:

$$W(r) = S^+ - S^- \tag{3.21}$$

$$W(r) = -\frac{(r - R_{in})}{R^*} - \frac{(r - R_{out})}{R^*} \tag{3.22}$$

$$W(r) = -\frac{(r - R^* + \triangle R_{in})}{R^*} - \frac{(r - R^* - R_{out})}{R^*} \tag{3.23}$$

Since $\triangle R_{in} = \triangle R_{out}$, $W(R^*) = 0$ justifying that $R^*$ is the equilibrium point or point of convergence.

**Theorem 1** *[70]: Consider the system $\dot{x} = f(x)$, with an equilibrium point $x = 0$. The origin is stable if and only if $xf(x) \leq 0$ in some neighborhood of the origin.*

It can be shown that, when $r < R^*$, $rW(r) > 0$ and when $r > R^*$, $rW(r) < 0$.

$$W(r) = -\frac{[r - (R^* - \triangle R_{in})]}{R^*} - \frac{[r - (R^* + \triangle R_{out})]}{R^*} \tag{3.24}$$

$$W(r) = -\frac{[r - R^* + \triangle R_{in})] - [r - R^* - \triangle R_{out})]}{R^*} \tag{3.25}$$

$$W(r) = \frac{-r + R^* - \triangle R_{in} - r + R^* + \triangle R_{out}}{R^*} \tag{3.26}$$

$$W(r) = -\frac{2(r - R^*)}{R^*} \tag{3.27}$$

Therefore,

$$rW(r) = -\frac{2r(r - R^*)}{R^*} \tag{3.28}$$

Note that, r is the weighted distance of an agents from the formation center and is never negative. The expression (3.28) is negative for $r > R^*$ and positive for $r < R^*$.

Therefore, $R^*$ is a stable point of convergence. Figure (3.7) supports this justification.

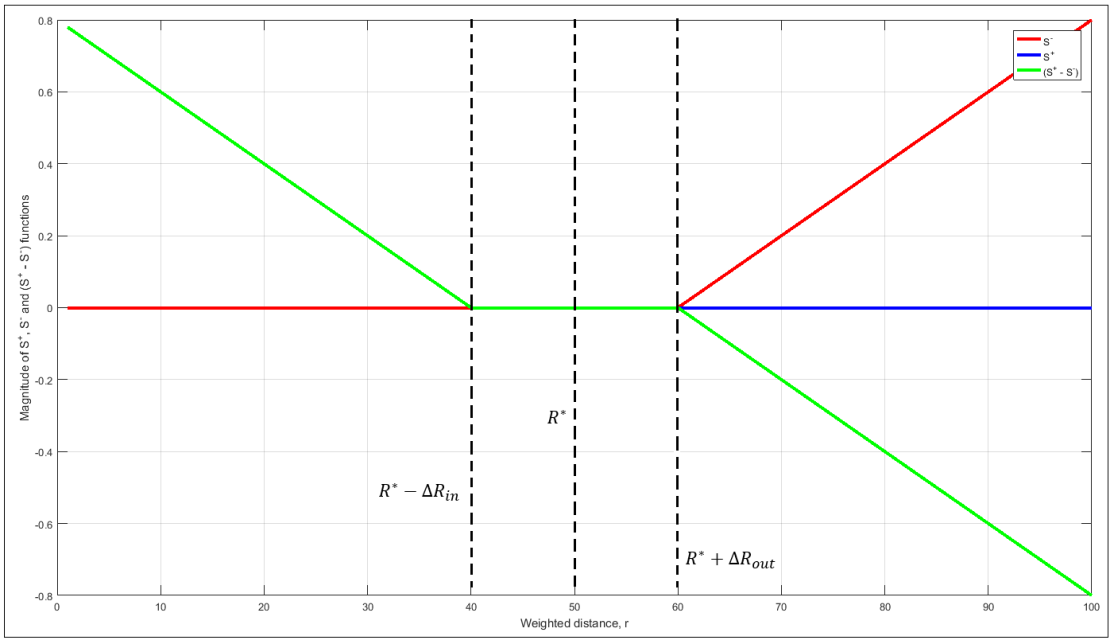


Figure 3.7: Behavior of $W(r)$ function (shown in green) in the $R^*$ neighborhood

## 3.5 Parameter Selection

Formation parameters are chosen based on basic geometry and logic. These selections must be made after considering the formation requirements such as number of agents, dimensions of each agent and desired shape of formation. Since the goal is to achieve a loose formation with agents lying between $R^* + \triangle R_{out}$ and $R^* - \triangle R_{in}$, there is some allowable error margin while selecting formation parameters. Guidelines for selecting formation control parameters are discussed below.

### 3.5.1 Selecting Principal Semi-Axes Ratio

The first necessary requirement is that the parameters $\gamma$ and $\lambda$ chosen must fit all the agents in the team (denoted by 'N'). These ratios also determine the shape of the

formation. If $\gamma < \lambda$, an oblate ellipsoid is obtained as in Figure (3.8b). If $\gamma > \lambda$, a prolate ellipsoid is obtained as in Figure (3.8a). If $\gamma = \lambda$, a sphere is obtained.

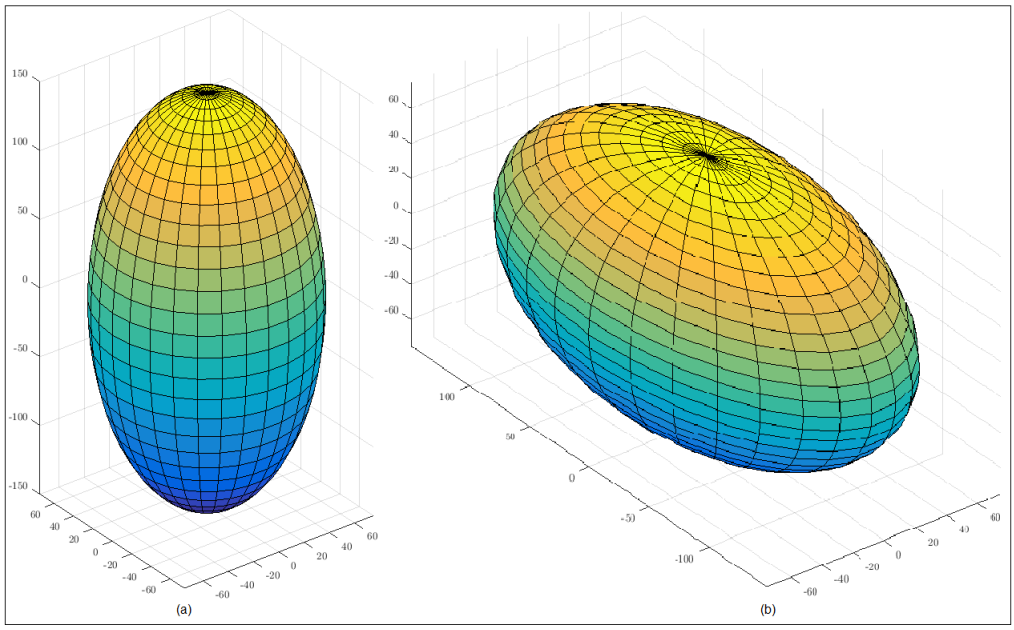


Figure 3.8: (a) Prolate ellipsoid (b) Oblate ellipsoid

### 3.5.2 Selecting $R^*$, $\triangle R_{out}$ and $\triangle R_{in}$

The radius of the ellipsoidal formation is chosen based on the desired size of the formation (denoted by 'N') and the dimensions of each agent. For a certain value of $R_{spacing}$ and $\triangle R_{avoid}$ if $R^*$ is chosen too large, the agents will be non-uniformly distributed in the $R^*$ neighborhood and if $R^*$ is chosen too small, some agents will be pushed outside the $R^*$ band. $\triangle R_{out}$ and $\triangle R_{in}$ define the radius of the outer and inner boundaries of the $R^*$ neighborhood. Decreasing $\triangle R_{out}$ and $\triangle R_{in}$ gives a tighter formation. However, if chosen too small the agents will have a zig-zag pattern along $R^*$ and if chosen too large they will have an offset pattern along $R^*$.

The maximum number of agents possible in a formation for fixed $R^*$ and $\triangle R_{avoid}$ parameters is:

$$N < \frac{4}{(0.5\triangle R_{avoid})^2}\left[\frac{(\frac{R^{*2}}{\gamma})^{1.6} + (\frac{R^{*2}}{\lambda})^{1.6} + (\frac{R^{*2}}{\gamma\lambda})^{1.6}}{3}\right]^{\frac{1}{1.6}} \tag{3.29}$$

# Chapter 4

# Results

The method described in Chapter 3 is demonstrated with simulations using MATLAB, where agents are considered as particles in the mission space. Parameters are selected based on the desired formation shape and the number of agents, as described in Section (3.5). The formation center $(x_c, y_c, z_c)$ is broadcast to all agents in the formation using which, each agent calculates a single velocity vector from the vector fields acting on it.

In this chapter simulations for ellipsoid and ellipsoid-like static and dynamic formations are performed. The number of agents chosen in each case is arbitrary. In order to efficiently demonstrate the working of the control algorithm, small number of agents are considered. The control algorithm works for larger number of agents, provided the dimensions of the formation ($R^*$) are appropriately chosen.

## 4.1 Simulations for Static Formation

### 4.1.1 Prolate Ellipsoidal Formation

Simulations for ten agents in an ellipsoidal formation are performed with the formation centered at the origin of world reference frame, and parameters used are shown

in Table (4.1). Additionally, the outer and inner ellipsoidal surfaces $R^* + \triangle R_{out}$ and $R^* - \triangle R_{in}$ respectively, are plotted in Figure (4.1) and a prolate ellipsoid formation is obtained by choosing $\gamma > \lambda$. Starting at random positions in mission space, Figure (4.1) shows the position of agents at different instances of time. It can be observed that the agents are attracted to the desired ellipsoidal area and disperse themselves within it.

For the same set of agents, the formation can be confined to a 2-dimensional plane (to obtain an ellipse/circle formation) by setting x, y or z planes to zero. Figures (4.2a), (4.2b) and (4.2c) show elliptical/circular formations in the y-z, x-z and x-y planes respectively, which are obtained by decreasing $R_{spacing}$ as the area enclosed by the formation is decreased. It is observed that the agents disperse themselves within the acceptable bands.

Table 4.1: Control Parameters for ten agents in Prolate Ellipsoid Formation

| Control Parameters | Ellipsoid Formation | Ellipse Formation |
|---|---|---|
| $R^*$ | 80 | 80 |
| $\triangle R_{in}$ | 5 | 5 |
| $\triangle R_{out}$ | 5 | 5 |
| $\gamma$ | 1 | 1 |
| $\lambda$ | 0.7 | 0.7 |
| $\triangle R_{avoid}$ | 5 | 5 |
| $R_{spacing}$ | 95 | 60 |

Figure (4.3) shows the change in weighted distance of agents 'r' from the center of formation with time, as they are attracted to the ellipsoidal band. It can be observed that, agents beginning from inside or outside the $R^*$ band reach the ellipsoidal region.

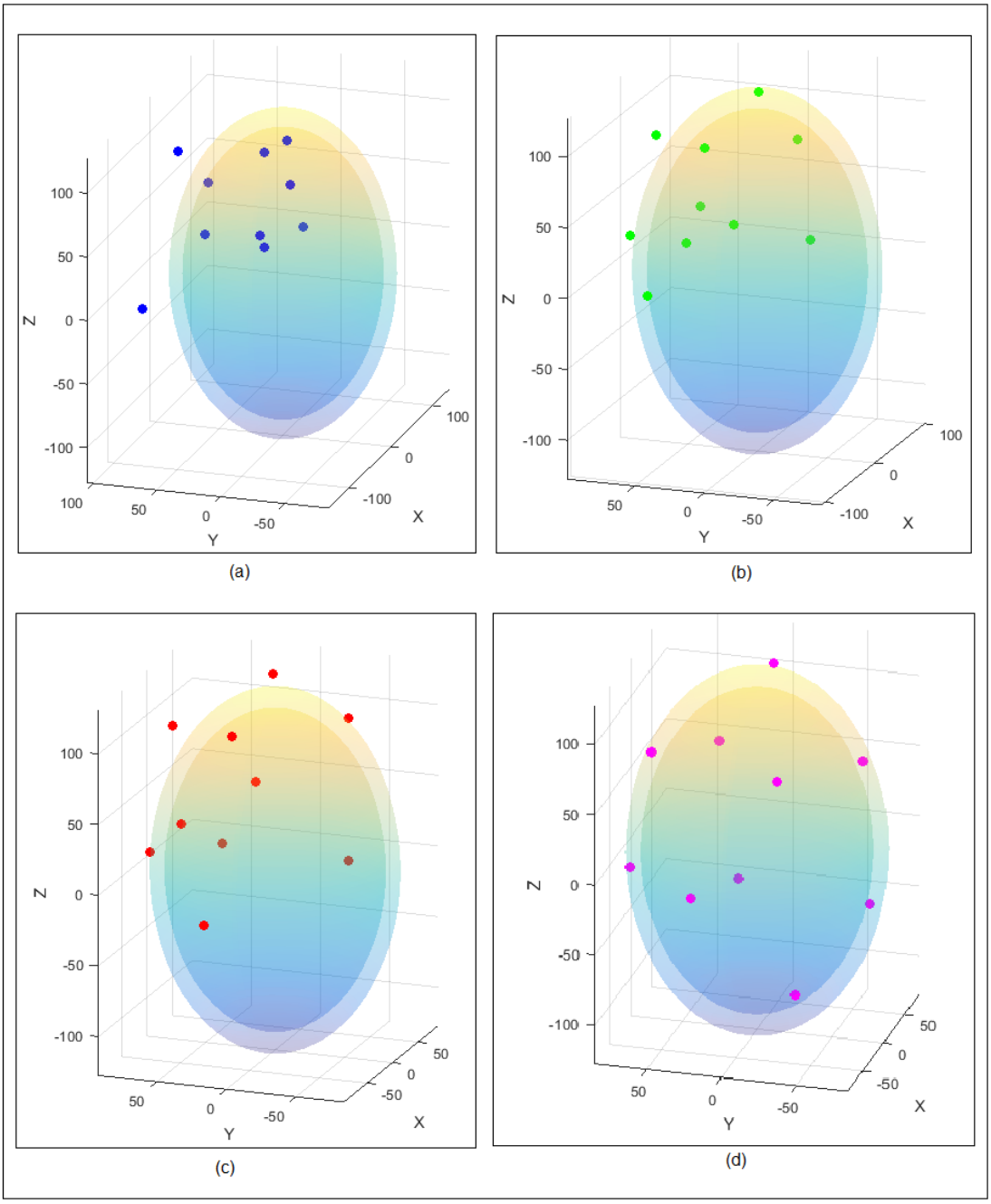


Figure 4.1: Ellipsoid formation of ten agents at (a) t=200 units (depicted in blue) (b) t=600 units (depicted in green) (c) t=1500 units (depicted in red) (d) t=10000 units (depicted in pink)

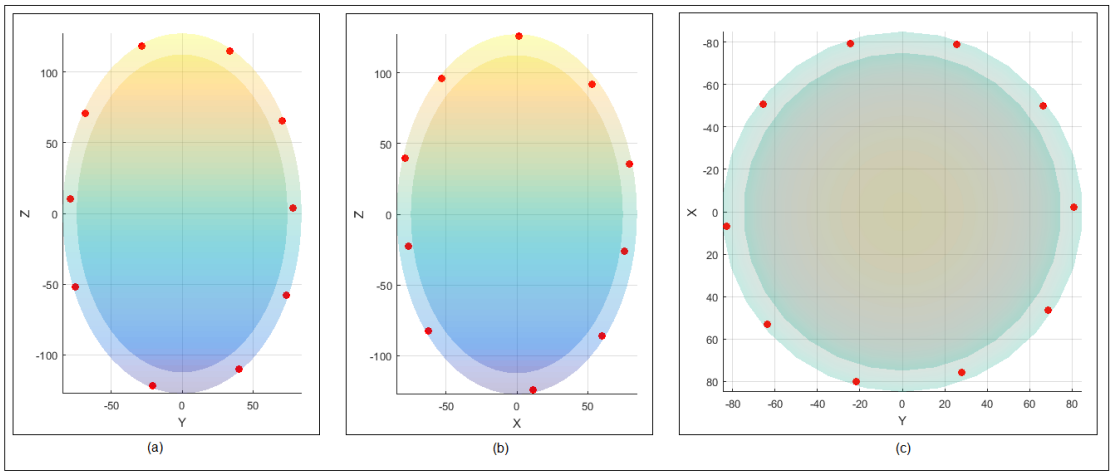


Figure 4.2: 2-D elliptical formation of ten agents with (a) X=0 (b) Y=0 (c) Z=0

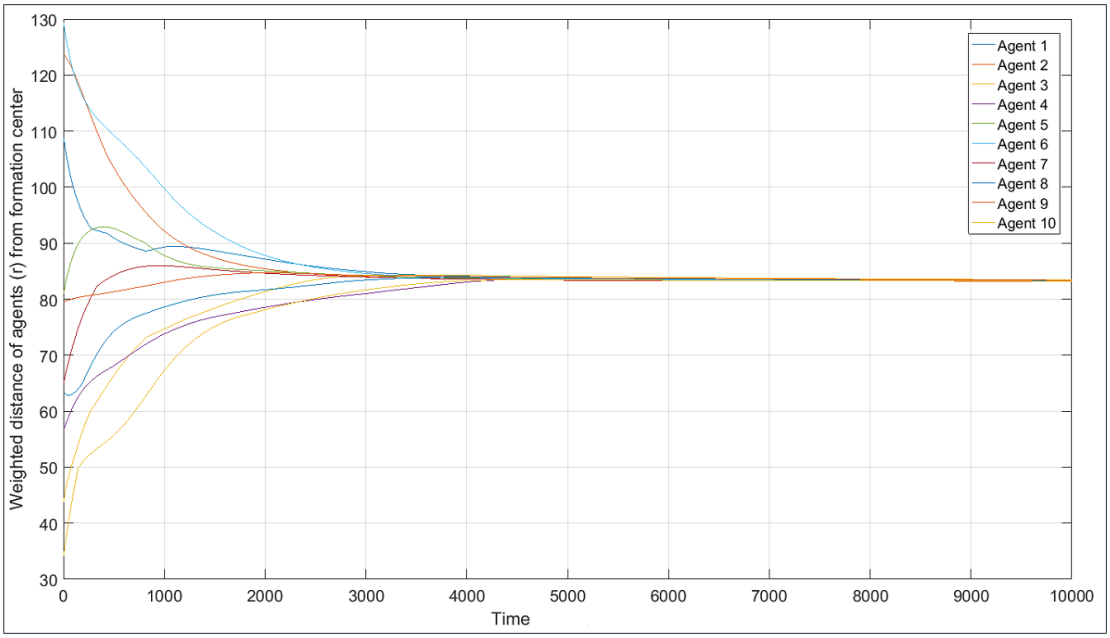


Figure 4.3: Weighted distance of ten agents from formation center for 3-D (prolate ellipsoid)

### 4.1.2 Oblate Ellipsoidal formation

Simulation of four agents in an oblate ellipsoid formation is performed which can be obtained by choosing the principal semi-axes ratios such that $\gamma < \lambda$. Other parameters

used for the simulation are shown in Table (4.2). Agents are attracted to the bounded ellipsoid area as shown in Figure (4.4), where the agent positions at initial $(t_0)$, intermediate $(t_1)$ and final $(t_2)$ time instances are plotted. Agents lying outside the ellipsoid are attracted to the bounded ellipsoid area due to the influence of the $G^+$ field and its corresponding limiting function $S^+$ while the agent lying inside the ellipsoid is pushed towards the bounded ellipsoid region by the influence of the $G^-$ vector fields and its limiting function $S^-$. The direction of motion of each agent is indicated in the plot. It can be observed that when an agent enters the agent avoidance or dispersion vector range of another agent, it experiences a change in orientation. All agents are attracted to the ellipsoid area and are dispersed within it.

Table 4.2: Control Parameters for four agents in Oblate Ellipsoid Formation

| Control Parameters | Ellipsoid Formation |
|---|---|
| $R^*$ | 80 |
| $\triangle R_{in}$ | 5 |
| $\triangle R_{out}$ | 5 |
| $\gamma$ | 1 |
| $\lambda$ | 2 |
| $\triangle R_{avoid}$ | 5 |
| $R_{spacing}$ | 110 |

Figure (4.5) shows the variation in weighted distance of four agents from center of formation. It is seen that agents are attracted to the $R^*$ neighborhood. Figure (4.6) plots inter-agent distances between four team members. The minimum distance between agents $(\triangle R_{avoid})$ is chosen as 5 units and the range for dispersion of agents $(R_{spacing})$

is chosen as 110 units. It can be observed from the plot that the inter-agent distances is greater than 110 units when the agents attain a formation. Thus, dispersion of agents in the ellipsoidal area is achieved.

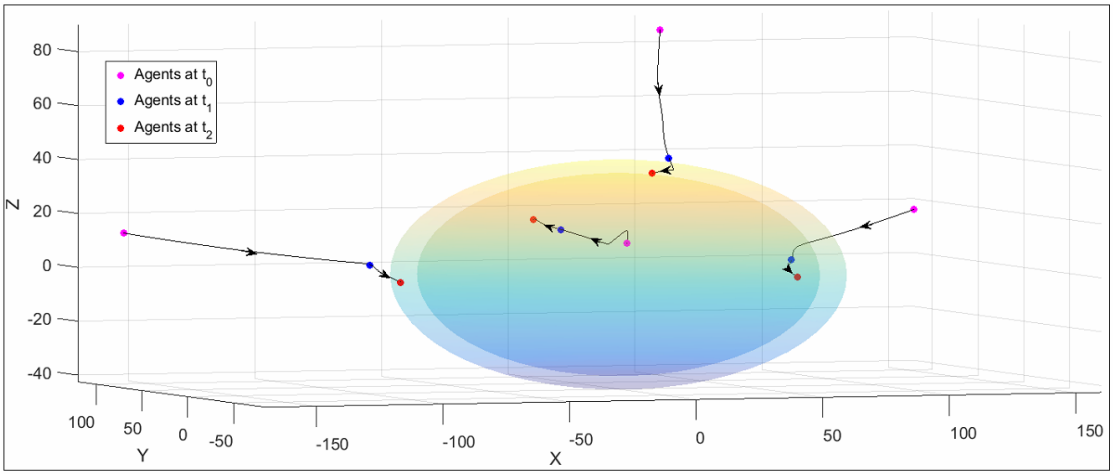


Figure 4.4: Agent positions at initial $(t_0)$, intermediate $(t_1)$ and final $(t_2)$ instances of time

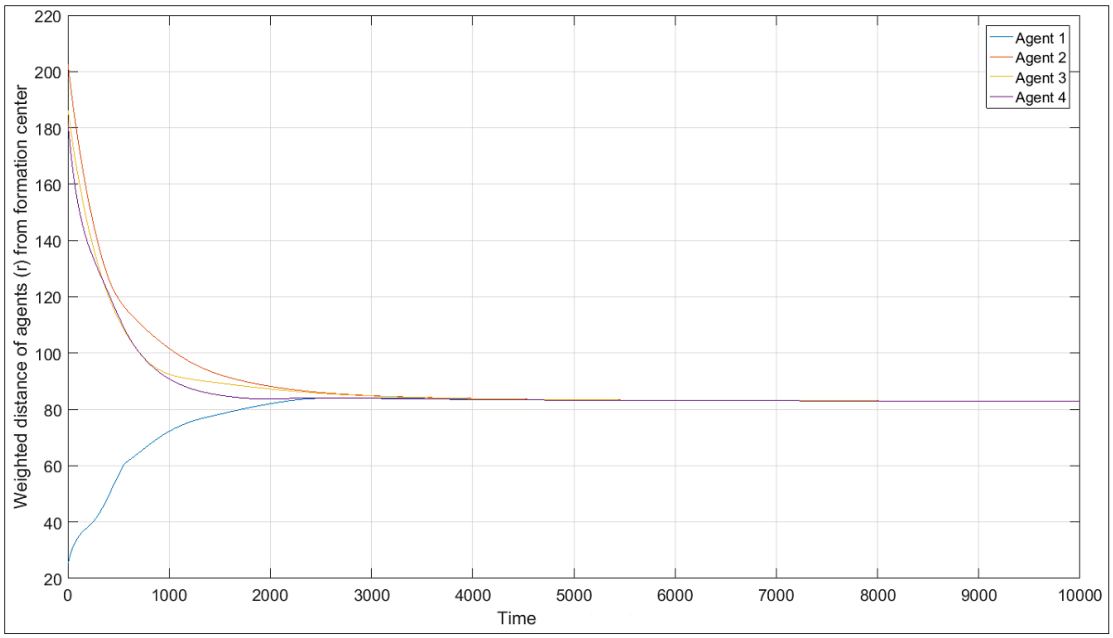


Figure 4.5: Weighted distance of four agents from formation center

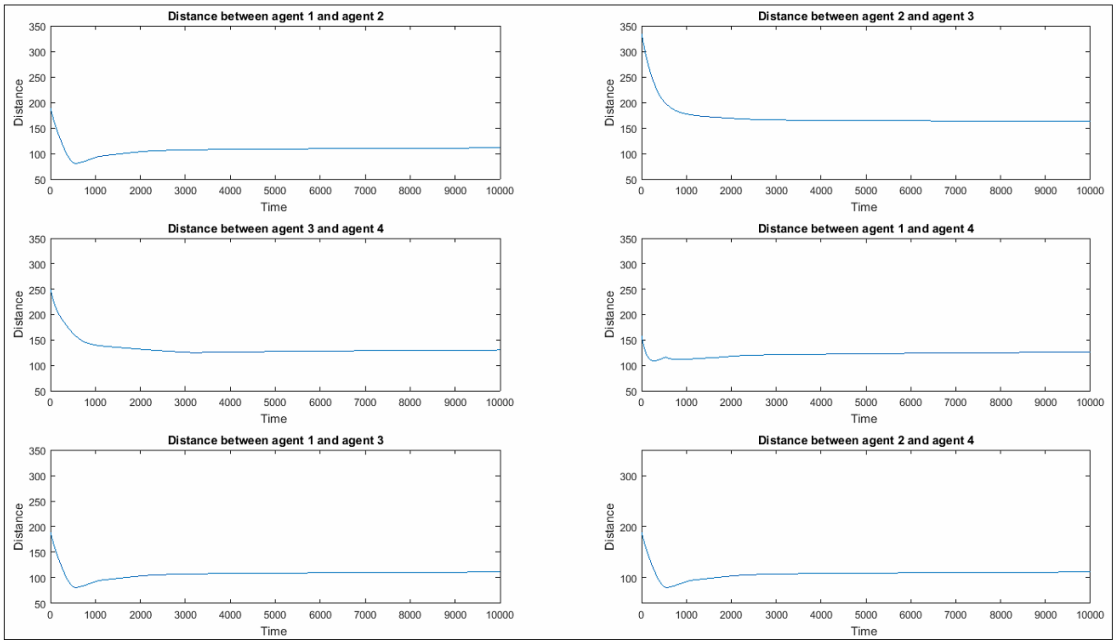


Figure 4.6: Distance between four agents in an ellipsoidal formation

### 4.1.3 Agents in a Spherical Formation

Table 4.3: Control Parameters for a sphere formation

| Control Parameters | Sphere Formation |
|---|---|
| $R^*$ | 80 |
| $\triangle R_{in}$ | 5 |
| $\triangle R_{out}$ | 5 |
| $\gamma$ | 1 |
| $\lambda$ | 1 |
| $\triangle R_{avoid}$ | 5 |
| $R_{spacing}$ | 95 |

Simulations are performed for a spherical formation and Table (4.3) shows the parameter values chosen. The only parameter that has to be changed to obtain a sphere

from an ellipsoid is $\gamma$ and $\lambda$, such that, $\gamma = \lambda$. Figure (4.7a) shows ten agents in a spherical formation. Figure (4.7b) shows a 'top view' of the formation where seven agents are visible and the other three agents that lie on the bottom surface of the sphere can be seen from the 'bottom view' in Figure (4.7c). All agents lie within the bounded sphere area.

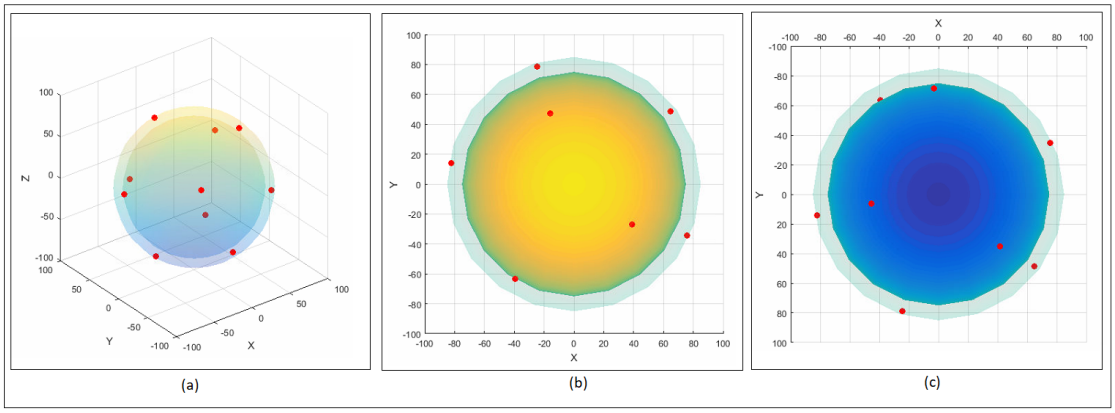


Figure 4.7: Spherical formation: (a) Ten agents in formation, (b) Top view of formation in part (a) is shown, (c) Bottom view of formation in part (a)

### 4.1.4 Agent Addition to Existing Formation

When a new agent is added, it's position is 'sensed' by the other agents, provided it is within a suitable range as described in Section (3.3.3). The new agent affects the collision avoidance and dispersion vector field of other agents, resulting in re-configuration of the existing formation. $R_{spacing}$ is decreased to accommodate the new agent.

Figure (4.8) shows a formation of four agents before a new agent is added. The agents move from their initial positions at time $t_0$ to an intermediate time step $t_1$ which is one time step before an agent is added. It can be observed that the agents disperse themselves within the ellipsoid area and are in formation at time $t_1$.

Table 4.4: Control Parameters for agent addition to a sphere formation

| Control Parameters | Sphere Formation |
|---|---|
| $R^*$ | 70 |
| $\triangle R_{in}$ | 5 |
| $\triangle R_{out}$ | 5 |
| $\gamma$ | 1 |
| $\lambda$ | 1 |
| $\triangle R_{avoid}$ | 15 |
| $R_{spacing}$ | 120 |

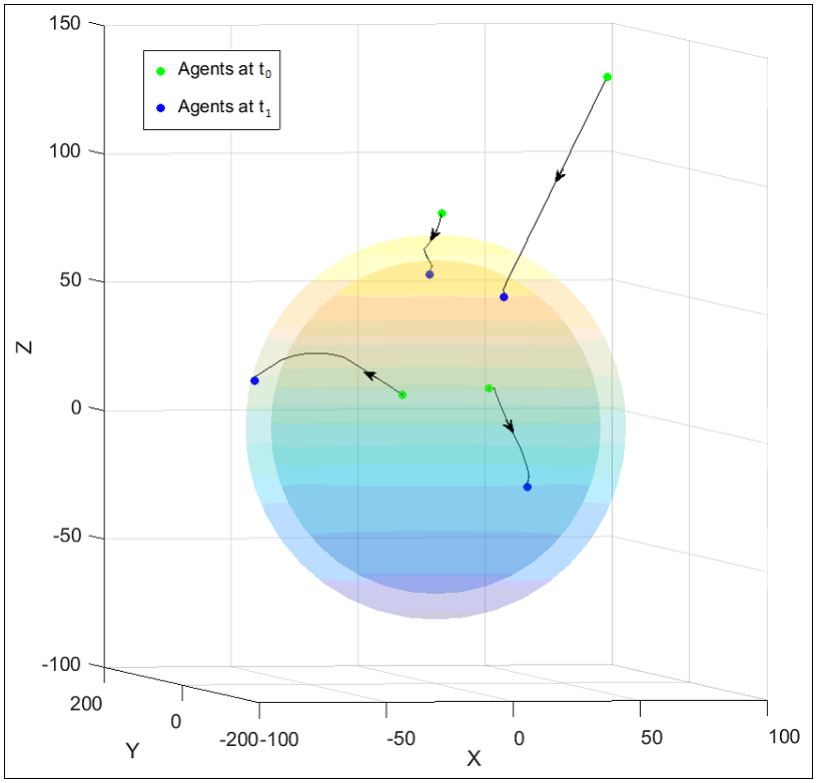


Figure 4.8: Formation of four agents with agent position at initial time ($t_0$) and at intermediate time ($t_1$) before addition of one agent

Figure (4.9) demonstrates re-configuration of the four existing agents to accommodate the new agent. Table (4.4) shows the parameter values chosen. The existing agents move within the ellipsoidal area while the new agent is attracted from outside the ellipsoid. The direction of motion of agents are indicated by arrows along their respective trajectories.

Figure (4.10) shows the variation of distances of four agents from the center of formation to accommodate the new agent. It is observed that, the new agent enters the formation at time t=1000 units and four existing agents move within the $R^*$ region to accommodate the new agent.

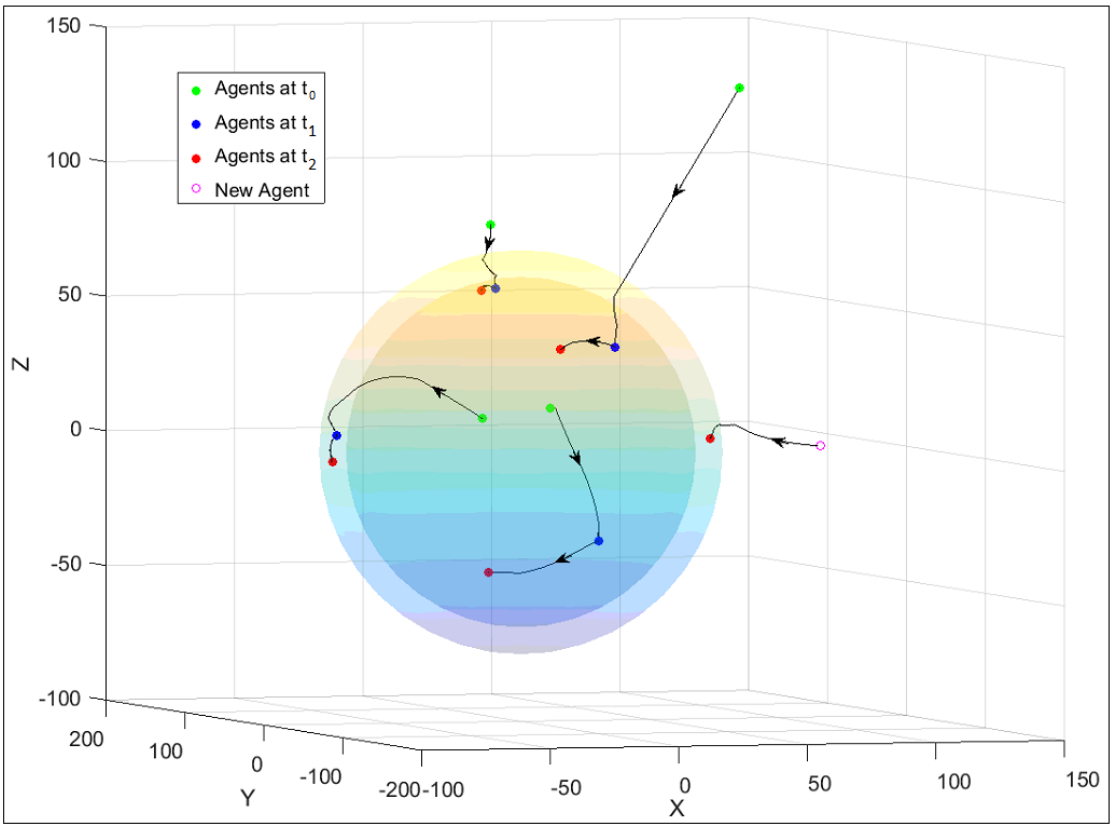


Figure 4.9: Formation of five agents at final time ($t_2$) where a new agent is added at time $t_1$

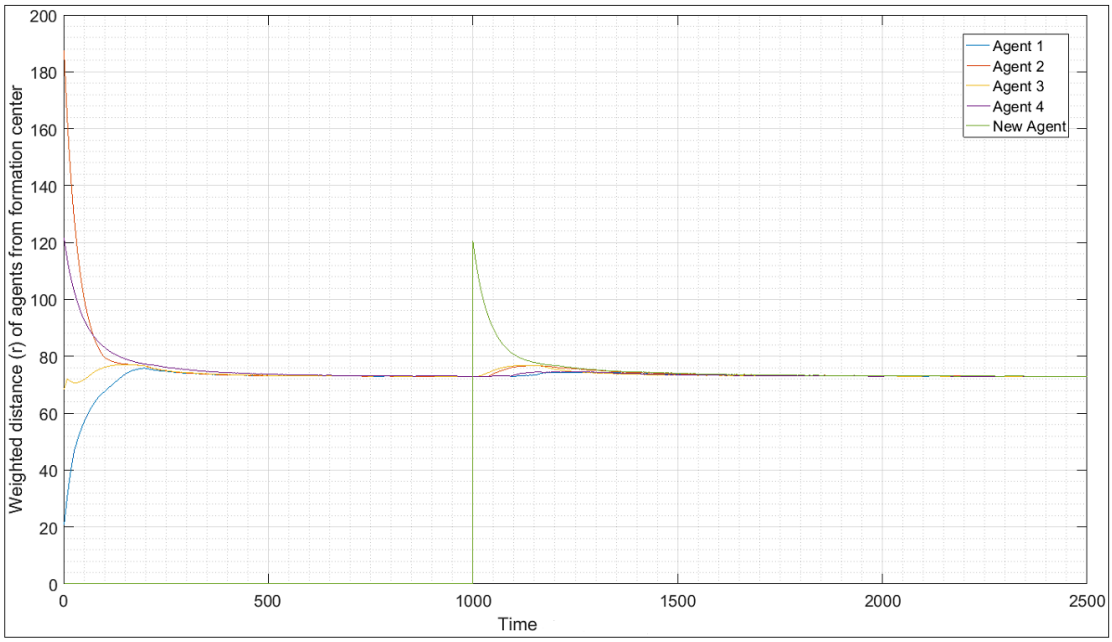


Figure 4.10: Distance of five agents from the center of formation

### 4.1.5 Agent Departure from Formation

Formation parameter values chosen are same as in Table (4.4) except that, $R_{spacing}$ is initially chosen as 100 units and is increased to 120 units to accommodate departure of an agent. Figures (4.11) shows formation of five agents where the agents are attracted to the bounded ellipsoid area from points outside and inside the ellipsoid. Position of agents at initial time $(t_0)$ and at one time step before departure of an agent $(t_1)$ is shown. The direction of motion of agents is denoted by arrows on their respective trajectories. Figure (4.12) show the formation after departure of one agent. The remaining four agents re-configure themselves.

Figure (4.13) shows variation of distances of five agents from the center of formation after re-configuration in the event of departure of one agent. Observe that, the remaining four agents move within the $R^*$ region at t=1000 units to re-configure themselves.

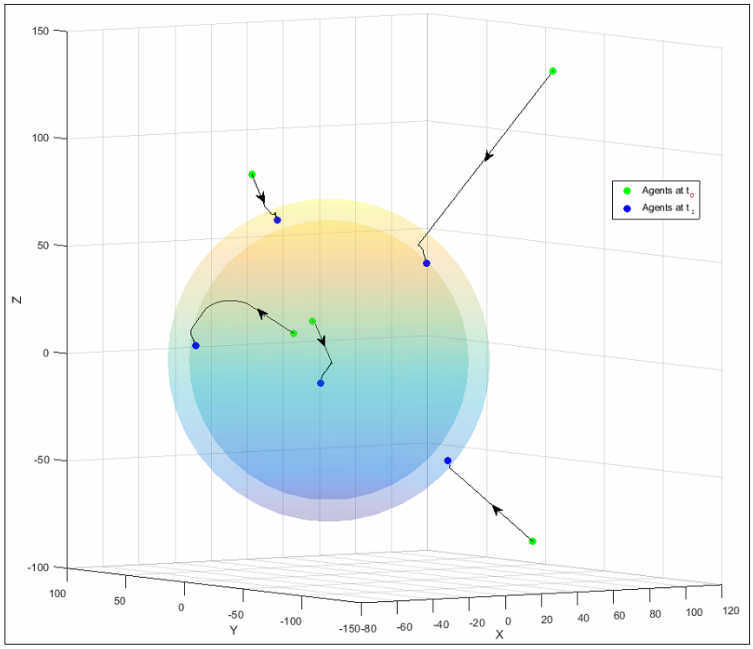


Figure 4.11: Formation of five agents at initial time $t_0$ and before departure of one agent ($t_1$)

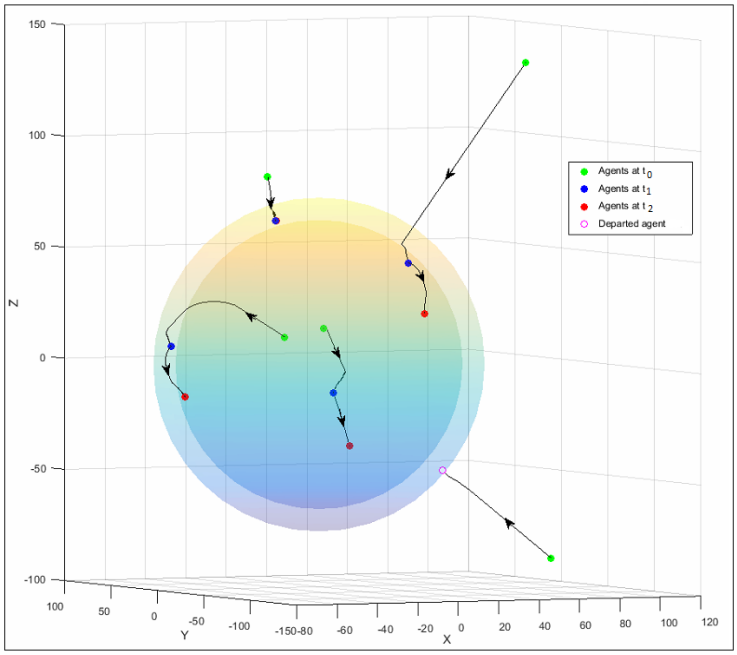


Figure 4.12: Formation of four agents at initial time $t_0$ and final time $t_2$ after departure of one agent

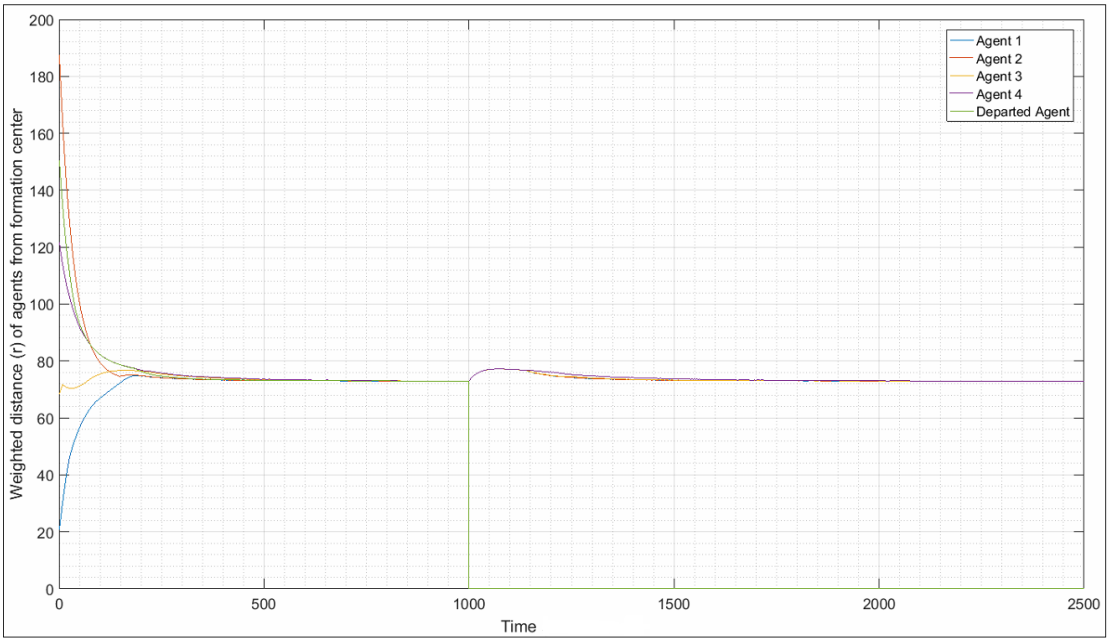


Figure 4.13: Distance of five agents from the center of formation with departure of one agent

## 4.2 Dynamic Formation

Table 4.5: Control Parameters for a dynamic sphere formation

| Control Parameters | Sphere Formation |
|---|---|
| $R^*$ | 70 |
| $\triangle R_{in}$ | 5 |
| $\triangle R_{out}$ | 5 |
| $\gamma$ | 1 |
| $\lambda$ | 1 |
| $\triangle R_{avoid}$ | 15 |
| $R_{spacing}$ | 105 |

Simulations are performed to demonstrate six agents following a trajectory in the x-y plane while maintaining a spherical formation. Control parameters used are listed in Table (4.5). The velocity vectors generated by each agent is relative to the center of formation. Therefore, the formation center $(x_c, y_c, z_c)$ shifts as a function of time and is updated as the agents move to obtain a dynamic formation. The only obstacles present in mission space are other agents.

Figure (4.14) illustrates a team of six agents following a trajectory in the x-y plane where agent positions at initial $(t_0)$, intermediate $(t_1)$ and final $(t_2)$ time steps are shown. Although the agents are continuously forced to re-orient themselves to follow the trajectory, they always remain within the bounded spherical formation.

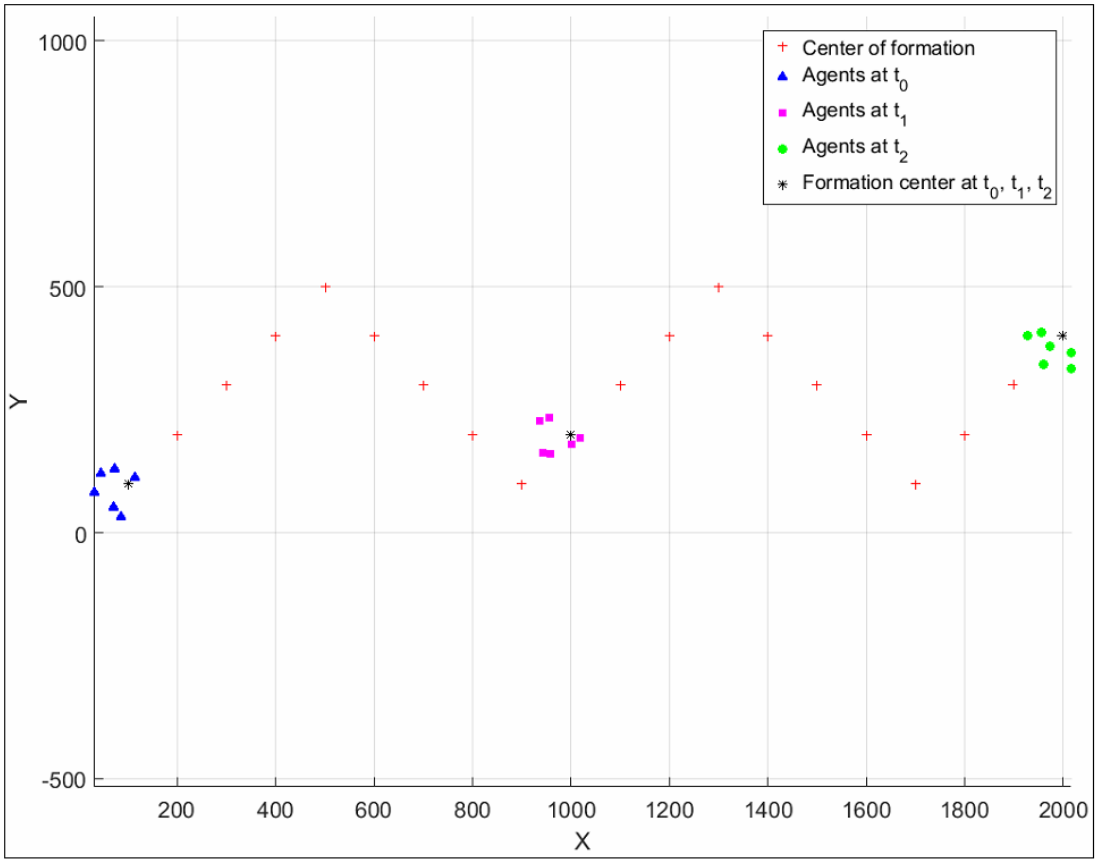


Figure 4.14: Spherical formation of six agents at initial $(t_0)$, intermediate $(t_1)$ and final $(t_f)$ time steps following a trajectory

Figure (4.15) illustrates the path traversed by each agent in the x-y plane relative to the center of formation. Agents beginning at random positions achieve and maintain a spherical formation while the agent avoidance vectors generated by each agent avoids inter-agent collisions. The entire formation does not move as a single unit along the trajectory, instead, velocity vectors are constantly generated by each agent as the center is shifted, resulting in continuous change in positions of the agents with respect to the formation center. The formation is continuously being re-configured and all agents take different time duration to reach their position in the formation.

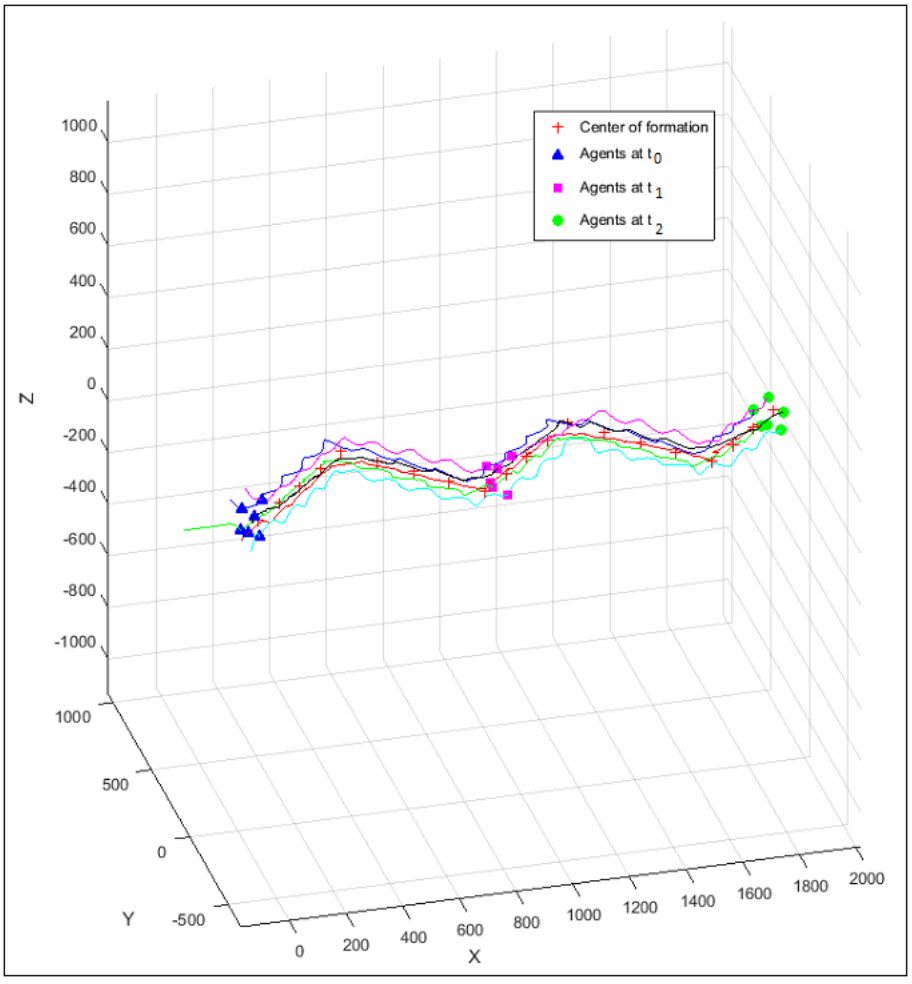


Figure 4.15: Trajectories of six agents maintaining a spherical formation

# Chapter 5

# Conclusion and Future Work

## 5.1 Conclusion

In this research, a control algorithm to attract a team of UAVs to a bounded ellipsoid/ ellipsoid-like formation is developed. Potential field vectors and limiting functions have been used to obtain a loose formation of UAVs which can avoid collisions, re-configure in the event of addition or departure of UAVs and move in the mission space while maintaining the formation.

The convergence of agents to the bounded ellipsoid region has been justified theoretically and simulations have been performed with particle agents to verify the accuracy of this method. A set of ellipsoid-like static formations are obtained by changing control parameters and the resulting formation is adaptable to addition or departure of team members. The formation can be scaled to larger team sizes by simply increasing the formation dimensions and a dynamic formation is achieved by shifting the formation center $(x_c, y_c, z_c)$ as a function of time. The advantage of this approach is the simplicity of vector generation and its adaptability to changes in formation shape and size.

## 5.2 Future Work

Although this research has produced important results, additional steps could be taken to improve the formation control algorithm. Controllers can be designed to tune the agent dispersion parameter to achieve better dispersion in the bounded ellipsoid area when agents depart or additional agents enter the formation. Agent position and velocity can be defined with respect to the global reference frame so that the formation can move as a single unit in the mission space.

# Bibliography


[1] L. E. Barnes, M. A. Fields, and K. P. Valavanis, "Swarm Formation Control Utilizing Elliptical Surfaces and Limiting Functions," *IEEE Transactions on Systems, Man and Cybernetics – Part B: Cybernetics, vol. 39, no. 6, pp. 1434-1445*, 2009.

[2] C. D. Rosales, M. Sarcinelli-Filho, G. Scaglia, and R. Carelli, "Formation Control of Unmanned Aerial Vehicles Based on the Null-Space", *International Conference on Unmanned Aircraft Systems, 2014, pp. 229-236*.

[3] D. Alejo, J. A. Cobano, G. Heredia, and A. Ollero,, "Particle Swarm Optimization for collision-free 4d Trajectory Planning in Unmanned Aerial Vehicles", *International Conference on Unmanned Aircraft Systems (ICUAS), 2013, pp. 298-307*.

[4] J. J. Corona-Sanchez, J. A. Vargas-Jacob, and H. Rodriguez-Cortes, "Decentralized real time implementation of a Leader-Follower coordination strategy for quadrotors", *International Conference on Unmanned Aircraft Systems (ICUAS), 2014, pp. 237-243*.

[5] S. Bereg, J. Diaz-Banez, M. Lopez, T. Rozario, and K. Valavanis, "A decentralized geometric approach for the formation keeping in unmanned aircraft navigation", *International Conference on Unmanned Aircraft Systems (ICUAS), 2015, pp. 989-997*.

[6] A. K. Das, R. Fierro, V. Kumar, J. P. Ostrowski, J. Spletzer, and C. J. Taylo, "A vision based formation control framework", *IEEE Transactions on Robotics and Automation, vol. 18, no. 2, 126-128*, 2017.

[7] W. L. Seng, J. C. Barca, and Y. A. Sekercioglu, "Distributed Formation Controlof Networked Mobile Robots in Environments with Obstacles". *[Online]. Available:https://www.cambridge.org/core/journals/robotica/article/distributed-formation-control-of-networked-mobile-robots-in-environments-with-obstacles/079F11C2425E19303F2987D%2041B6E5AAC*.

[8] K. A. Ghamry and Y. Zhang, "Formation Control of Multiple Quadrotors Based on Leader-Follower Method", *International Conference on Unmanned Aircraft Systems (ICUAS), 2015, pp. 1037-1042*.

[9] Y. Kim and H. Bang, "Decentralized Control of Multiple Unmanned Aircraft for Target Tracking and Obstacle avoidance", *International Conference on Unmanned Aircraft Systems (ICUAS), 2016, pp. 327-331*.

[10] L. V. Santana, A. S. Brandao, and M. Sarcinelli-Filho, "Heterogeneous Leader-Follower Formation based on Kinematic Models", *International Conference on Unmanned Aircraft Systems (ICUAS), 2016, pp. 342-346*.

[11] R. Fierro, A. K. Das, V. Kumar, and J. P. Ostrowski, "Hybrid Control of Formations of Robots", *International Conference on Robotics and Automation, 2001, pp. 157-162*.

[12] Z. X. Liu, X. Yu, C. Yuan, and Y. M. Zhang, "Leader-Follower Formation Control of Unmanned Aerial Vehicles with Fault Tolerant and Collision Avoidance Capabilities", *International Conference on Unmanned Aircraft Systems (ICUAS), 2015, pp. 1025-1030*.

[13] J. P. Desai, J. P. Ostrowski, and V. Kumar, "Modeling and Control of Formations of Nonholonomic Mobile robots", *IEEE Transactions on Robotics And Automation,vol. 17, no. 6, pp. 905-908*, 2001.

[14] Z. Chao, S.-L. Zhou, L. Ming, and W.-G. Zhang, "UAV Formation Flight Basedon Nonlinear Model Predictive control", *Mathematical Problems in Engineering, vol. 2012, Article ID 261367, 15 pages*, 2012.

[15] G. Merrill and C. Becker, "Formation Flying for Satellites and UAVs". *[Online]. Available:https://ntrs.nasa.gov/archive/nasa/casi.ntrs.nasa.gov/20150016267.pdf*.

[16] F. Liang, F. Wang, X. Zhao, and Y. Hou, "Distance-based control of formations with hybrid communication topology: Three-agent case", *IEEE Advanced Information Management, Communicates, Electronic and Automation Control Conference (IMCEC), 2016, pp. 1910-1915*.

[17] J. Nielsen and R. Sharma, "Formation Control of Quadrotor UAVs using a Single Camera", *International Conference on Unmanned Aircraft Systems (ICUAS), 2015, pp. 18-25*.

[18] M. Whitzer, J. Keller, S. Bhattacharya, V. Kumar, T. Sands, L. R. A. Pope, and D. Dickmann, "In-flight Formation Control for a Team of Fixed-Wing Aerial Vehicles", *International Conference on Unmanned Aircraft Systems (ICUAS), 2016, pp. 372-380*.

[19] J. P. Desai, J. Ostrowski, and V. Kumar, "Controlling formation of multiple mobile robots", *International Conference on Robotics and Automation, 1998, pp. 2864-2869*.

[20] P. Tabuada, G. J. Pappas, and P. Lima, "Motion Feasibility of Multi-Agent Formations", *IEEE Transactions on Robotics, vol. 21, no. 3, pp. 387-392*, 2005.

[21] T. Paul, T. R. Krogstad, and J. T. Gravdahl, "Modelling of UAV formation flight using 3D potential field", *Simulation Modelling Practice and Theory, vol. 16, pp. 1453-1462*, 2008.

[22] J. A. Guerrero and R. Lozano, *Flight Formation Control. ISTE Ltd. and John Wiley & Sons, Inc., 2012, ISBN: 9781848213234*.

[23] M. Bunic and S. Bogdan, "Potential function based multi-agent formation control in 3d space", *10th IFAC Symposium on Robot Control International Federation of Automatic Control, 2012, pp. 682-689*.

[24] A. Franchi, C. Masone, V. Grabe, M. Ryll, H. H. Bulthoff, and P. R. Giordano, "Modeling and control of uav bearing-formations with bilateral high-level steering", *The International Journal of Robotics Research, vol. 31, no. 12, pp. 1504-1525*, 2012.

[25] Y. Deng, K. Qin, and G. Xie,, "3-D space flight formation control for UAVs based on MAS", *Journal of Theoretical and Applied Information Technology, vol. 47, no. 2,pp. 1504-1525*, 2013.

[26] V. Rezaei and M. Stefanovic, "Distributed leaderless and leader-follower consensus of linear multiagent systems under persistent disturbances", *24th Mediterranean Conference on Control and Automation (MED), 2016, pp. 587-592*.

[27] R. G. Braga, R. C. da Silva, A. C. B. Ramos, and F. Mora-Camino, "A combined approach for 3D formation control in a multi-uav system using ROS", *International Micro Air Vehicle Conference and Flight Competition (IMAV), 2017, pp. 196-202*.

[28] P. U. Lima, A. Ahmad, A. Dias, A. G. S. Conceicao, A. P. Mpreira, E. Silva,L. Almeida, L. Oliveria, and T. P. Mascimento, "Formation control driven by cooperative object tracking", *Robotics and Autonomous Systems, vol. 63, pp. 68-79, 2015*.

[29] D. V. Zarzhitsky, P. DeLima, and D. J. Pack, "Localizing stationary targets withcooperative unmanned aerial vehicles", *IFAC Workshop on Networked Robotics,2009, pp. 68-73*.

[30] S. Kumbasar and O. Tekinalp, "Fuzzy logic guidance of formation flight", *International Conference on Unmanned Aircraft Systems (ICUAS), 2015, pp. 167-175*.

[31] A. Ahmad and P. Lima, "Multi-robot cooperative spherical-object tracking in 3d space based on particle filters", *Robotics and Autonomous Systems, vol. 61,pp. 1084-1093, 2013*.

[32] H. G. Tanner and A. Kumar, "Towards decentralization of multi-robot navigationfunctions", *IEEE International Conference on Robotics and Automation (ICRA),2005, pp. 4132-4137*.

[33] P. Song and R. V. Kumar, "A potential field based approach to multi-robot manipulation", *IEEE International Conference on Robotics and Automation (ICRA),2002, pp. 1217-1222*.

[34] L. M. Wachter, J. Murphy, and L. E. Ray, "Potential function control for multiple high-speed nonholonomic robots", *IEEE International Conference on Robotics and Automation (ICRA), 2008, pp. 1781-1782*.

[35] R. Gayle, W. Moss, M. C. Lin, and D. Manoch, "Multi-robot coordination using generalized social potential fields", *IEEE International Conference on Robotics and Automation (ICRA), 2009, pp. 106-113*.

[36] H. Rezaee and F. Abdollahi, "Adaptive artificial potential field approach for obstacle avoidance of unmanned aircrafts", *IEEE/ASME International Conference on Advanced Intelligent Mechatronics, 2012*.

[37] W. Kang, N. Xi, Y. Zhao, J. Tan, and Y. Wang, "Formation control of multipleautonomous vehicles: Theory and experimentation", *Proceedings of IFAC 15th Triennial World Congress, 2002*.

[38] J. Buhmann, W. Burgard, A. B. Cremers, D. Fox, T. Hofmann, F. E. Schneider,J. Strikos, and S. Thrun, "The mobile robot rhino", *AI Magazine, vol. 16, no. 2,pp. 31-38, 1995*.

[39] Y. Sakagami, R. Watanabe, C. Aoyama, S. Matsunaga, N. Higaki, and K. Fujimura, "The intelligent asimo: System overview and integration", *In Proceedings of IROS'02, 2002, pp. 2478-2483*.

[40] http://marsrover.nasa.gov/home/index.html

[41] M. Raibert, K. Blankespoor, G. Nelson, R. Playter, and the BigDog Team, "Bigdog, the rough-terrain quadruped robot", *In Proceedings of the 17th World Congress of the International Federation of Automatic Control, 2008, pp. 10822-10825*.

[42] D. Gouaillier, V. Hugel, P. Blazevic, C. Kilner, J. Monceaux, P. Lafourcade, B.Marnier, J. Serre, and B. Maisonnier, "Mechatronic design of nao humanoid", *In Proceedings of ICRA'09, 2009, pp. 769-774*.

[43] J. Wawerla and R. T. Vaughan, "A fast and frugal method for team-task allocation in a multirobot transportation system", *In Proceedings of ICRA'10, 2010, pp. 1432-1437*.

[44] Z. Yan, N. Jouandeau, and A. A. Cherif, "Multi-robot heuristic goods transportation", *In Proceedings of IS'12, 2012*.

[45] D. A. Shell and M. J. Mataric, "On foraging strategies for large-scale multi-robot systems", *2006 IEEE/RSJ International Conference on Intelligent Robots and Systems, 2006, pp. 2717-2723*.

[46] H. Liu, N. Stoll, S. Junginger, and K. Thurow, "Mobile robotic transportation in laboratory automation: Multi-robot control, robot-door integration and robot-human interaction", *2014 IEEE International Conference on Robotics and Biomimetics (ROBIO 2014), pp. 1033-1038*.

[47] Y. Dai, Y. Kim, S. Wee, D. Lee, and S. Lee, "Symmetric caging formation for convex polygonal object transportation by multiple mobile robots based on fuzzy sliding mode control", *ISA Transactions, vol. 60, pp. 321-332, 2016*.

[48] R. Zlot, A. Stentz, M. B. Dias, and S. Thaye, "Multi-robot exploration controlled by a market economy", *In Proceedings of ICRA'02, May 2002, pp. 3016-3023*.

[49] W. Sheng, Q. Yang, S. Ci, and N. Xi, "Multi-robot area exploration with limited-range communications", *In Proceedings of IROS'04, September 2004, pp. 1414-1419*.

[50] L. Wu, M. A. Garcia, D. Puig, and A. Sole, "Voronoi-based space partitioning for coordinated multi-robot exploration", *Journal of Physical Agents, vol. 1, no. 1,pp. 37-44, September 2007*.

[51] D. A. Lima and G. M. Oliveira, " A cellular automata ant memory model of foraging in a swarm of robots", *Applied Mathematical Modelling, vol. 47, pp. 551-572, July 2017*.

[52] http://www.robocup.org.

[53] http://www.grappa.univ-lille3.fr/icga.

[54] N. Michael, J. Fink, and R. V. Kumar, "Cooperative manipulation and transportation with aerial robots", *Auton. Robots, vol. 30, pp. 73-86, 2011*.

[55] A. Benzerrouk, L. Adouane, and P. Martinet, "Stable navigation in formation for a multi-robot system based on a constrained virtual structure", *Robotics and Autonomous Systems, vol. 62, pp. 1806-1815, December 2014*.

[56] W. Ren and N. Sorensen, "Distributed coordination architecture for multi-robot formation control", *Robotics and Autonomous Systems (2007), August 2007*.

[57] K.H. Tan and M. A. Lewis, "Virtual structures for high-precision cooperative mobile robotic control", *Proceedings of the IEEE/RSJ International Conference on Intelligent Robots and Systems, 1996, pp. 132-139*.

[58] https://www.liquid- robotics.com/about- us/company/company-history/.

[59] https://www.nasa.gov/centers/ames/news/releases/2004/psa/psa.html.

[60] https://phys.org/news/2018-02-humanoid-robot-emergency-response-teams.html.

[61] N. Y. Law, Y. C. Kwong, J. J. Q. Lee, K. H. Kwok, Z. L. Lam, Y. Yue, K. L. Man,and C.-U. Lei, "Derrt: Disastrous emergency response robot team for cooperative rescue", *Proceedings of the International Multi Conference of Engineers and Computer Scientists 2014 Vol II, March 2014*.

[62] M. Langerwisch, T. Wittmann, S. Thamke, T. Remmersmann, A. Tiderko, and B. Wagner, "Heterogeneous teams of unmanned ground and aerial robots for reconnaissance and surveillance - a field experiment", *2013 IEEE International Symposium on Safety, Security, and Rescue Robotics (SSRR), Linkoping 2013, pp. 1-6*.

[63] A. Stoica, T. Theodoridis, H. Hu, K. McDonald-Maier, and D. F. Barrero, "Towards human-friendly efficient control of multi-robot teams", *2013 International Conference on Collaboration Technologies and Systems (CTS), San Diego, CA,2013, pp. 226-231*.

[64] T. Sun, H. Pei, Y. Pan, H. Zhou, and C. Zhang, "Neural network-based sliding mode adaptive control for robot manipulators", *Neurocomputing, vol. 47, no. 14, pp. 2377-2384, 2011*.

[65] J. Xu, M. Wang, and L. Qiao, "Dynamical sliding mode control for the trajectory tracking of under actuated unmanned underwater vehicles", *Ocean Engineering, vol. 105, pp. 54-63, 2015*.

[66] Thilagavathi.P, Naveena.T, Manjuparkave.A.R, Sridhar.C, and Mathankumar.R, "Land survobot for measuring land values and soil quality", *Asian Journal of Applied Science and Technology (AJAST), vol. 2, no. 2, pp. 557-562, April-June 2018*.

[67] *https://store.irobot.com/default/roomba-vacuuming-robot-vacuum-irobot-roomba-i7-7150/i715020.html?-ga=2.257866829.719060508.1557278460-1415136594.1556523487&-gac=1.36884500.1557278460.EAIaIQobChMI2-3i7OKK4gIVFb3sCh17ng4eEAAYASAAEgJYx_D_BwE*.

[68] R. C. Luo, W. U. Chan, and P. Lai, "Intelligent robot photographer: Help people taking pictures using their own camera", *2014 IEEE/SICE International Symposium on System Integration, Tokyo, 2014, pp. 322-327*.

[69] *https : / / www . egr . msu . edu / k̃halil / NonlinearControl /Slides-Short/Lecture_2.pdf*.